2.

NUREG/CR-4195
EGG-2380
November 1985

Overview of TRAC-PD2 Assessment Calculations

Michael E. Waterman

F O R M A L R E P O R T

EG&G Idaho

Work performed under
DOE Contract No. DE-AC07-76ID01570
for the ***U.S. Nuclear Regulatory Commission***

Idaho National Engineering Laboratory

Managed by the U.S. Department of Energy

Available from

Superintendent of Documents
U.S. Government Printing Office
Post Office Box 37082
Washington, D.C. 20013-7982

and

National Technical Information Service
Springfield, VA 22161

NOTICE

DISCLAIMER

NUREG/CR-4195
EGG-2380
Distribution Category: R4

NUREG/CR--4195

TI86 003980

OVERVIEW OF TRAC-PD2 ASSESSMENT CALCULATIONS

Michael E. Waterman

Published November 1985

EG&G Idaho, Inc.
Idaho Falls, Idaho 83415

Prepared for the
Division of Accident Evaluation
Office of Nuclear Regulatory Research
U.S. Nuclear Regulatory Commission
Washington, D.C. 20555
Under DOE Contract No. DE-AC07-76IDO1570
FIN No. A6047

ABSTRACT

A summary of Transient Reactor Analysis Code Version PD2 (TRAC-PD2) calculations performed at the Idaho National Engineering Laboratory (INEL) is presented in this report as part of the U.S. Nuclear Regulatory Commission's (NRCs) overall assessment program of TRAC-PD2. The calculated and measured parameters summarized in this report are break mass flow rate, primary coolant system pressure, reactor core flow rates, and fuel rod cladding temperatures. The data were obtained from seven tests that were performed at two test facilities. The tests were conducted to study the various aspects of cold leg break transients, including the effects of large and small breaks, and core reflood phenomena. User experience gained from the various calculations is also summarized.

FIN A6047—Code Assessment and Applications (Transients).

SUMMARY

This report summarizes seven TRAC-PD2 calculations that were performed at the Idaho National Engineering Laboratory (INEL) and reported between November and December of 1981. An overview of selected results is provided herein as a referenceable document of that work.

The criteria used to assess the calculational capabilities of TRAC-PD2 were based on accurately simulating break flow rate response, primary system pressure response, core flow response, and cladding temperature response. Large- and small-break loss-of-coolant accidents (LOCAs) were considered.

The seven calculations were of three large-break loss-of-coolant-accident (LBLOCA) tests performed in the Semiscale Mod-1 facility (located at the INEL), two small-break loss-of-coolant-accident (SBLOCA) tests performed in the Semiscale Mod-3 facility, and two reflood tests performed in the Kraftwerk Union primary coolant loop (PKL) test facility in Erlangen, West Germany, and the Semiscale Mod-3 facility. An eighth test (LOC-11C) was conducted in the Power Burst Facility at the INEL, but the data from this LBLOCA test were not comprehensive enough to allow adequate modeling of the break downstream conditions. Consequently, an accurate assessment of the LOC-11C break flow response was not possible, which is important in the calculation of other system parameters. Therefore, the results of the TRAC-PD2 assessment of Test LOC-11C will not be included in this report.

Conclusions regarding the TRAC-PD2 analyses are:

1. TRAC-PD2 calculated the LBLOCA primary system responses reasonably well based upon the criteria used in this report. It is therefore considered adequate for LBLOCA calculations. However, primary system mass distribution was not adequately calculated in the small-break calculations, which had an adverse effect on other important parameters. Consequently, use of TRAC-PD2 for SBLOCA calculations is not recommended.

2. In general, differences between calculated and measured break flow rates caused differences between the TRAC-PD2 results and the measured data. Calculated break flow rates that were higher than measured break flows resulted in higher rates of depressurization. This, in turn, led to early emergency core coolant (ECC) injection and, subsequently, earlier times of cladding quench.

   The TRAC-PD2 newsletter suggested that the break nozzle be nodalized with 17 cells. This recommendation was not followed in at least four of the seven calculations. It is recommended that users of TRAC-PD2 perform some sensitivity analyses of break flow nodalization prior to committing substantial resources to the calculation.

   When the calculated break flow was the same as the measured flow rate, the primary system pressure response was in reasonable agreement with the measured data. This indicated that the primary system pressure response would have been representative of the measured response.

3. Calculated pressure response trends were generally adequate, given the inaccuracy of calculated break flow rate responses. The primary coolant system pressure responses were calculated reasonably well in the single-phase portions of the blowdowns (subcooled and saturated steam with throat void fractions near 100%). Pressures during the two-phase depressurization period were generally poorly calculated, due to problems in modeling the correct break plane geometry. The calculated system pressures were ∿55% higher than the measured pressures during the two-phase blowdown period.

4. Core flow calculations were generally adequate, although there were some inaccuracies in the time of lower plenum refill and core reflood. These inaccuracies were caused by inaccurate break flow responses. Better modeling of the break nozzle should result in improved calculated system responses.

5. The mean calculated peak cladding temperature deviation from measured data was -19.8 K ± 23.8 K. There was reasonable agreement of time of reflood and quench, and the presence or absence of critical heat flux (CHF) was generally well calculated, as were both top-down and bottom-up quenches. The material properties used for the electrically heated Semiscale fuel rods were not available in the TRAC-PD2 material properties package. This problem caused some discrepancies in the fuel rod temperature responses. Additionally, calculated three-dimensional effects in the core were not verified by the test data. Sensitivity calculations should be performed when initializing the core model to insure reasonable predictions of core flow response.

6. Limited computer run time statistics were available for four of the seven calculations (refer to Section 4). The ratio of CPU time to transient time varied from 13:1 to 295:1, depending on the complexity of the model and the transient type. The high ratios occurred during the reflood portion of the calculations.

Improvements that are needed include:

1. TRAC-PD2 calculations of condensation events are generally inaccurate and overemphasized. Further work on this model would result in better calculations of core flow response and cladding temperature response.

Recommendations regarding the use of TRAC-PD2 are:

1. The user should perform sensitivity calculations to determine the best nodalization for a break nozzle. The TRAC-PD2 newsletter suggests 17 nodes as an optimal value. The break nozzle should be able to reasonably calculate single-phase flow response. Two-phase break flow data are generally difficult to accurately measure; consequently, these data should not be used to define the break nozzle nodalization.

2. TRAC-PD2 can explicitly or semi-explicitly calculate conditions in the vessel. The user should use the semi-implicit method instead of performing a direct inversion solution of the vessel matrix. The calculated results will be the same, and the run time will be less.

3. The Iloeje correlation for the departure from nucleate boiling (DNB) temperature should be used during the refill portion of the transient when the core is completely voided. The cladding surface temperatures are not significantly affected by this correlation during this phase, and the cost of the calculation can be reduced by approximately 50% during this phase. The homogeneous nucleation minimum temperature should be used during the core reflood phase.

A summary of the user experience gained from the various calculations (refer to Section 5) provides methods for performing a calculation with more efficiency than would otherwise occur by strictly using the TRAC-PD2 input manual.

CONTENTS

The following appendixes are on microfiche cards attached to the back inside cover of this report.

FIGURES

TABLES

OVERVIEW OF TRAC-PD2 ASSESSMENT CALCULATIONS

1. INTRODUCTION

The purpose of this report is to provide an overview of the results of seven TRAC-PD2 calculations that were performed at the INEL and reported between November and December of 1981, and to provide a single referenceable document of that work. The summarized reports are included as appendices to this report.

Certain criteria have been selected to determine the TRAC-PD2 capabilities in calculating loss-of-coolant accidents (LOCAs). The criteria selected for this assessment report are:

1. Break flow rate response. Accurate calculation of break flow rate response is important, because the primary coolant system pressure is a function of the amount of mass in the system. If the calculated break flow rate is higher than the measured break flow rate, the calculated primary system pressure will be lower than the measured pressure, which will in turn influence the timing of important system events, such as emergency core coolant (ECC) injection and time of cladding quench.

2. Primary system pressure response. The primary system pressure response must be accurately calculated, or those system events related to pressure will not be adequately addressed in the calculation.

3. Core flow rate response. An accurate calculation of core flow rate response is necessary in determining what the temperature response will be in the core, because core temperature is dependent on the core liquid mass distribution.

4. Cladding temperature response. The purpose of calculating LOCAs is to determine analytically the probability of core fuel damage caused by excessive cladding temperatures. The calculation of the correct cladding temperatures is essentially the bottom line for any code designed to calculate a LOCA. If the peak cladding temperatures cannot be accurately calculated, the code cannot be judged adequate.

The seven calculations were of three large-break loss-of-coolant-accident (LBLOCA) tests performed in the Semiscale Mod-1 facility (located at the INEL), two small-break loss-of-coolant-accident (SBLOCA) tests performed in the Semiscale Mod-3 facility, and two reflood tests performed in the Kraftwerk Union primary coolant loop (PKL) test facility in Erlangen, West Germany, and the Semiscale Mod-3 facility. An eighth test, Power Burst Facility Test LOC-11C, was evaluated, but the initial conditions were not accurately modeled; consequently, the results of the LOC-11C calculation could not be used for TRAC-PD2 assessment.

Test K5A was a reflood test performed in the KWU PKL test facility. The main objective of the test was to study the refill and reflood response of the electrically heated core. The TRAC-PD2 calculation covered the first 300 s of the test.

Test S-04-5 was a LBLOCA test performed in the Semiscale Mod-1 test facility. The main objective of the test was to study the integral blowdown-reflood response of the Semiscale Mod-1 system. The TRAC-PD2 calculation covered the first 167 s of the test.

Semiscale Mod-1 Tests S-28-1 and S-28-10 were LBLOCA tests with steam generator tube rupture occurring 40 s and 60 s after the break, respectively. The difference between the tests was in the timing of the simulated tube ruptures and in the number of tube ruptures. Test S-28-1 represented a rupture of 60 tubes initiated 40 s after the LOCA, while Test S-28-10 represented a smaller rupture of 12 tubes initiated 60 s after the rupture. The main objective of this test series was to determine the range of steam generator tube ruptures over which high peak cladding temperatures could be expected to occur. The TRAC-PD2 calculations simulated the first 60 s for Test S-28-1 and the first 120 s of Test S-28-10.

Test S-07-4 was a reflood test performed in the Semiscale Mod-3 test facility. The main objective of the test was to study reflood phenomena in the core. The TRAC-PD2 calculation simulated the first 100 s of the test.

Semiscale Mod-3 Tests S-SB-2A and S-SB-4 were SBLOCA tests. The tests simulated 2.5% cold leg breaks in a pressurized water reactor (PWR) and in the Loss of Fluid Test (LOFT) facility, respectively. Additionally, the break was not isolated from the steam generator in Test S-SB-2A, as it was in S-SB-4. The TRAC-PD2 calculations simulated the first 1500 s in Test S-SB-2A, and the first 1260 s in Test S-SB-4.

A summary of the test identifications, facilities, and test objectives is provided in Table 1.

A brief description of the test facilities that were modeled for the various calculations is presented in Section 2. TRAC-PD2 calculated data and test data regarding break flow response, primary system coolant pressure response, core flow response, and cladding temperature response are compared in Section 3. A brief table of computer run time statistics is in Section 4. Conclusions regarding the prediction of selected responses are presented in Section 5. User experiences regarding the use of TRAC-PD2 are summarized in Section 6. The summarized reports are provided in Appendixes A through E.

Table 1. Test description summary

Test ID	Facility	Type of Test
K5A	KWU PKL	Refill and reflood phase of LBLOCA
S-04-5	Semiscale Mod-1	Integral blowdown-reflood of Semiscale Mod-1 system
S-28-1	Semiscale Mod-1	Large-break LOCA with 60 ruptured steam generator tubes
S-28-10	Semiscale Mod-1	Large-break LOCA with 12 ruptured steam generator tubes
S-07-4	Semiscale Mod-3	Reflood phase of LBLOCA
S-SB-2A	Semiscale Mod-3	SBLOCA simulation of a PWR
S-SB-4	Semiscale Mod-3	SBLOCA simulation of LOFT Test L3-1
LOC-11C	Power Burst Facility	LBLOCA

2. TEST FACILITIES, MODELS, AND TEST DESCRIPTIONS

A brief description of the test facilities that were modeled for the calculations is provided in this section. The facilities that were modeled are the Semiscale Facility, located at the INEL, and the Primary Coolant Loop test facility (PKL) located in West Germany. More detailed information regarding these facilities may be obtained from the various appendixes. Brief descriptions of the TRAC-PD2 models and a summary of the various tests are also included in this section.

2.1 Description of the PKL Test Facility and TRAC-PD2 Model

The PKL facility was designed to represent a four-loop West German 1300-MW B1BL1S-B PWR. The prototype volume-to-power ratio was maintained in the 340-rod experimental design. Consequently, the nominal scaling factor of 1:134 was the ratio of the number of rods in the experimental core to the corresponding prototype. The rods were electrically heated.

The four primary coolant loops of the prototype were simulated in the experiment using three loops: two intact loops and one loop containing a break simulation. One of the intact loops was representative of two of the prototype loops. The loop arrangement is shown in Figure 1. Each of the loops contained an operating steam generator and a simulated pump volume with a variable resistance. The core contained 340 electrically heated rods with a total available power of 1.45 MW.

The PKL facility was modeled with 26 components and 28 junctions. Included in the model were the pressure vessel, the three loops and steam generators, the simulated pumps, the ECC injection ports, the downcomer pipe, and the bypass steam line. Nodalizations of the TRAC-PD2 model are shown in Figures 2 and 3.

More detailed information is provided in Appendix A.

2.2 Description of the Semiscale Mod-1 Test Facility and TRAC-PD2 Model

The Semiscale Mod-1 system and instrumentation for the cold leg break configuration are shown in Figure 4. This system was a 1:1705 scale model of a typical four-loop Westinghouse PWR. It consisted of a pressure vessel with simulated reactor internals (downcomer, lower plenum, core, and upper plenum); an intact loop with a pressurizer, steam generator, active pump, and associated piping; a broken loop with a simulated steam generator, simulated pump, associated piping, and break assemblies; a pressure suppression system with a header and suppression tank; and a coolant injection system with high- and low-pressure injection pumps and an accumulator. The core region contained 40 1.68-m electrically heated rods that were 0.011 m in diameter.

Nodalization diagrams of the Semiscale Mod-1 system and vessel for the S-04-5 test and S-28-1 and S-28-10 tests are shown in Figures 5 and 6 and Figures 7 and 8, respectively. The major differences in the two TRAC-PD2 models of the Semiscale Mod-1 system were the addition of the junction in the intact loop to simulate steam generator tube rupture mass contributions in the S-28 tests, and changes in the circumferential nodalization of the vessel components.

Further details regarding the Semiscale Mod-1 facility and the TRAC-PD2 models are available in Appendixes B and C.

2.3 Description of the Semiscale Mod-3 Test Facility and TRAC-PD2 Model

The Semiscale Mod-3 test facility was a modification of the Mod-1 facility described in the previous section. An isometric drawing of the facility is shown in Figure 9. The Mod-3 system consisted of a vessel with its associated internal components, an external downcomer, and active intact and broken loops with their associated components.

The intact loop contained an active steam generator and pump and associated piping. The pressurizer was connected to this loop during reflood experiments. The broken loop contained an active steam generator, an active pump, and a break simulator.

The Mod-3 vessel consisted of an upper head, upper plenum with simulated internal components, electrically heated core region, lower plenum, and

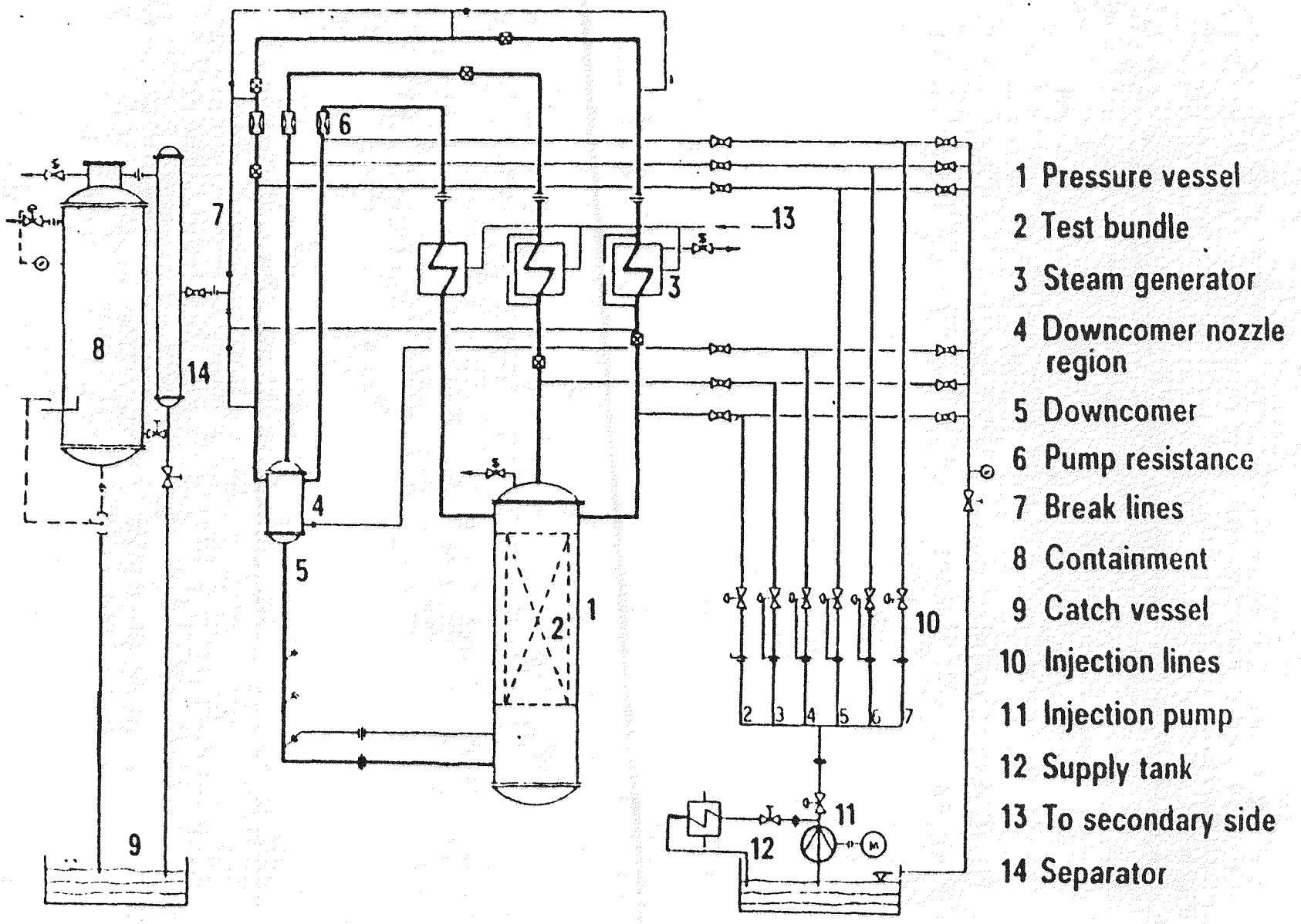

Figure 1. KWU PKL test facility.

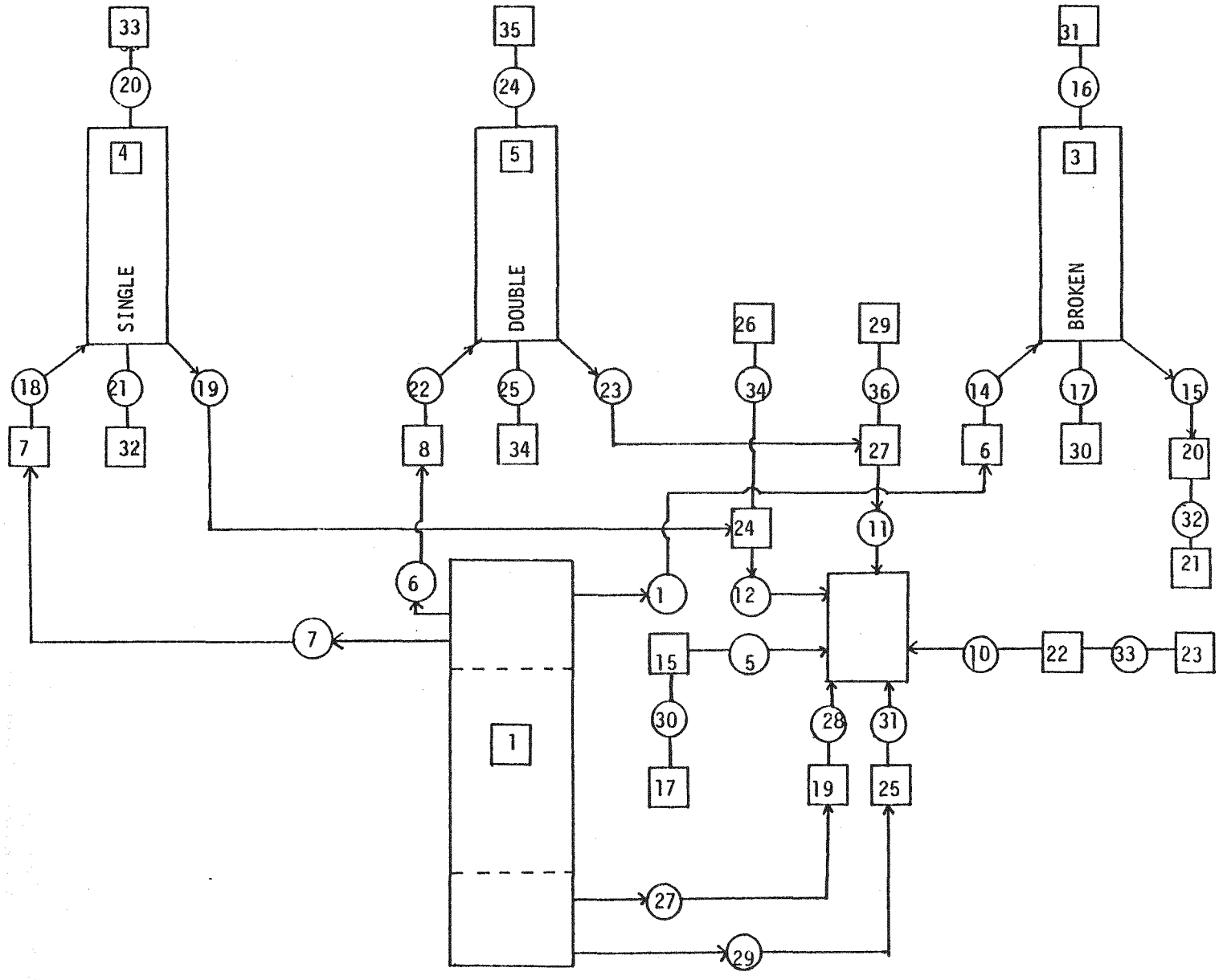

Figure 2. TRAC-PD2 model of the KWU PKL test facility.

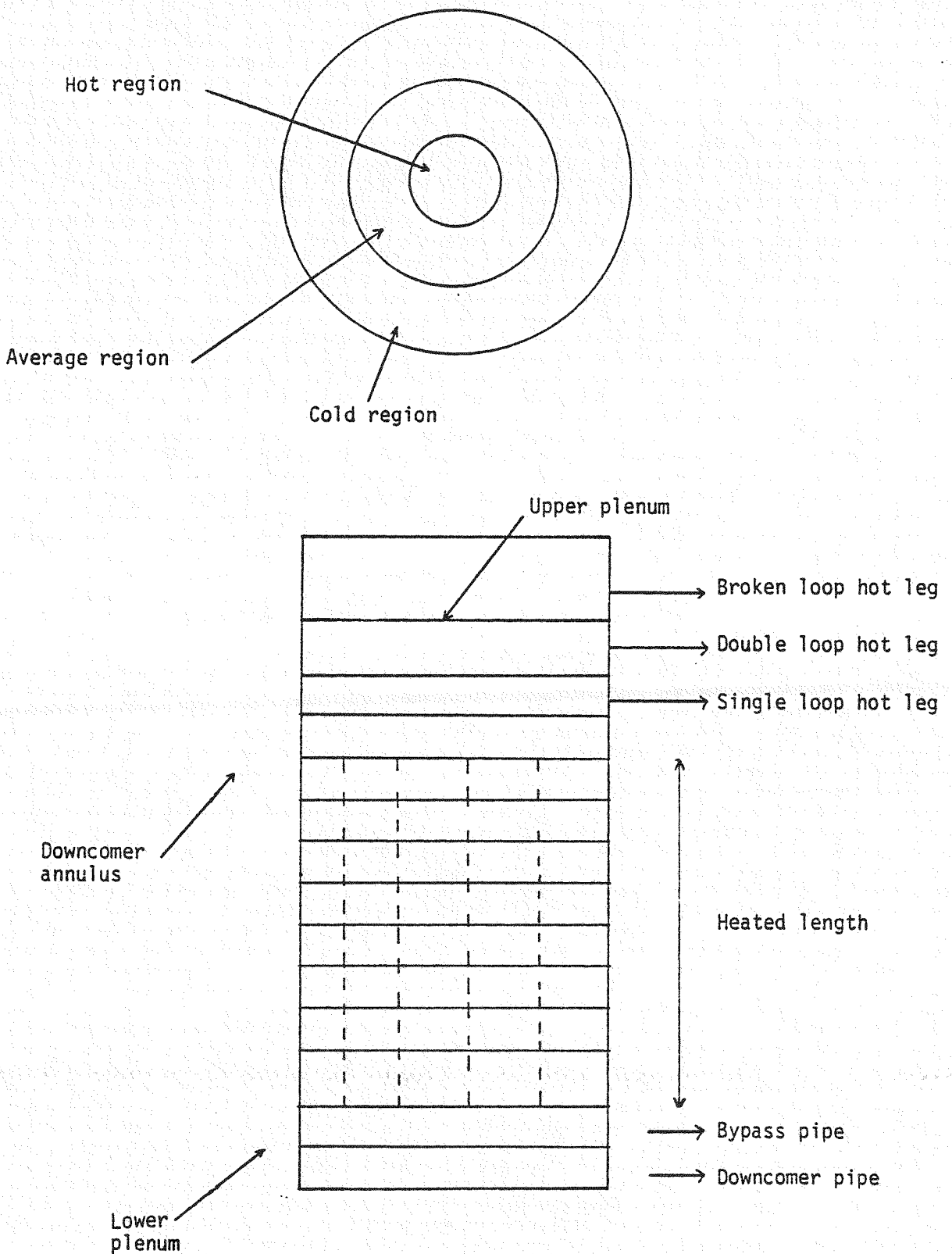

Figure 3. TRAC-PD2 model of the PKL vessel.

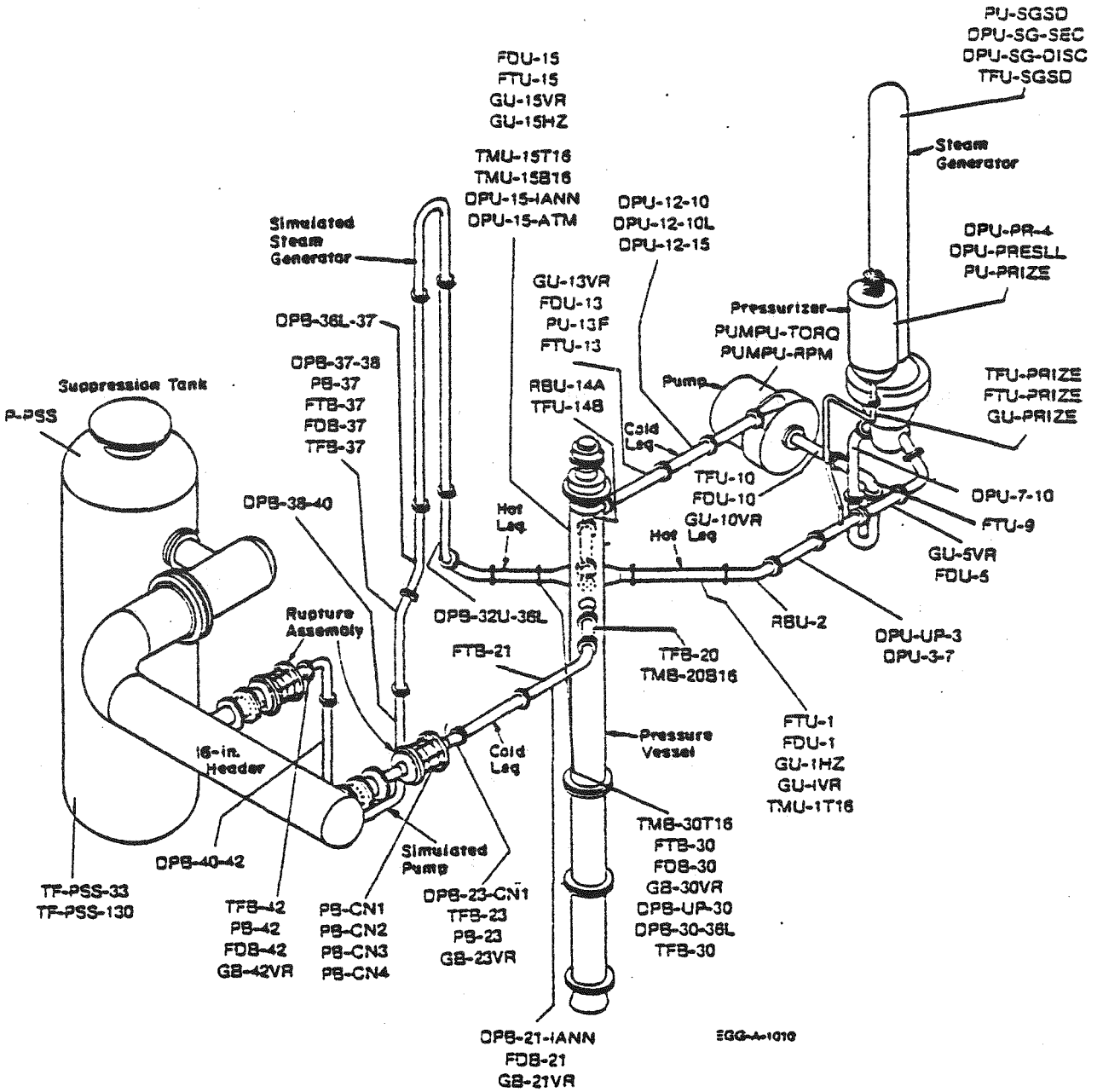

Figure 4. Semiscale Mod-1 test facility.

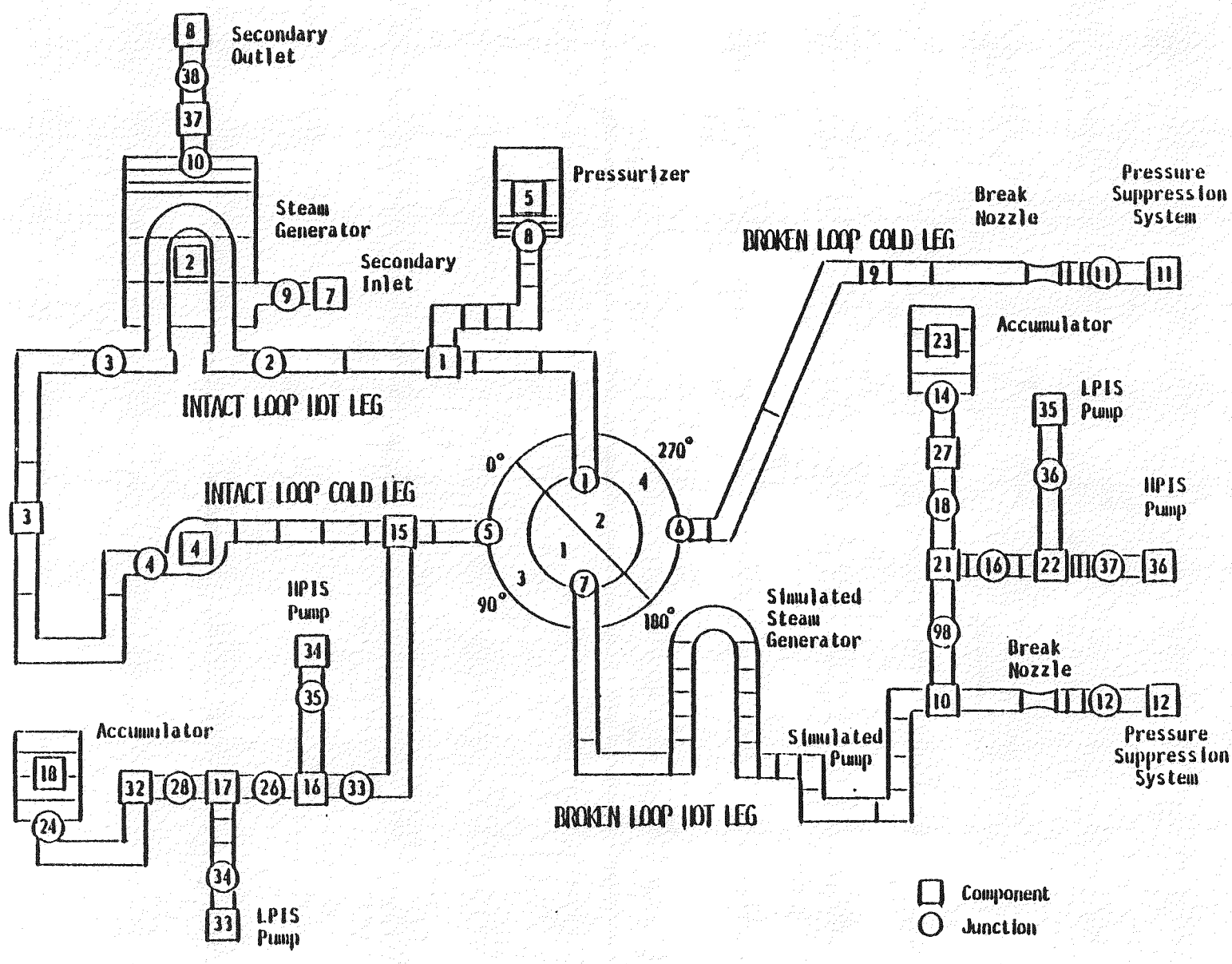

Figure 5. TRAC-PD2 model of the Semiscale Mod-1 test facility for Test S-04-5.

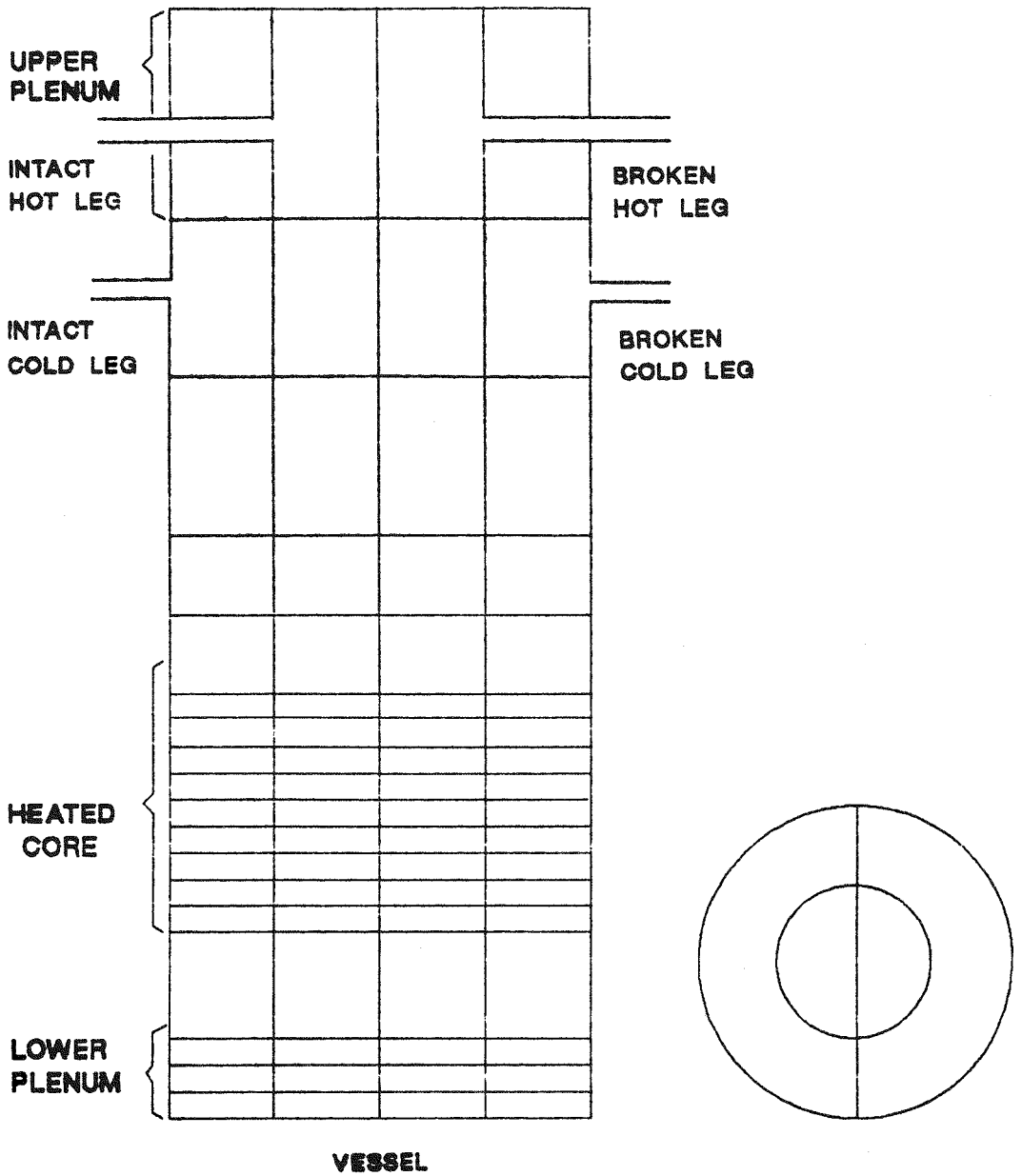

Figure 6. TRAC-PD2 model of the Semiscale Mod-1 vessel for Test S-04-5.

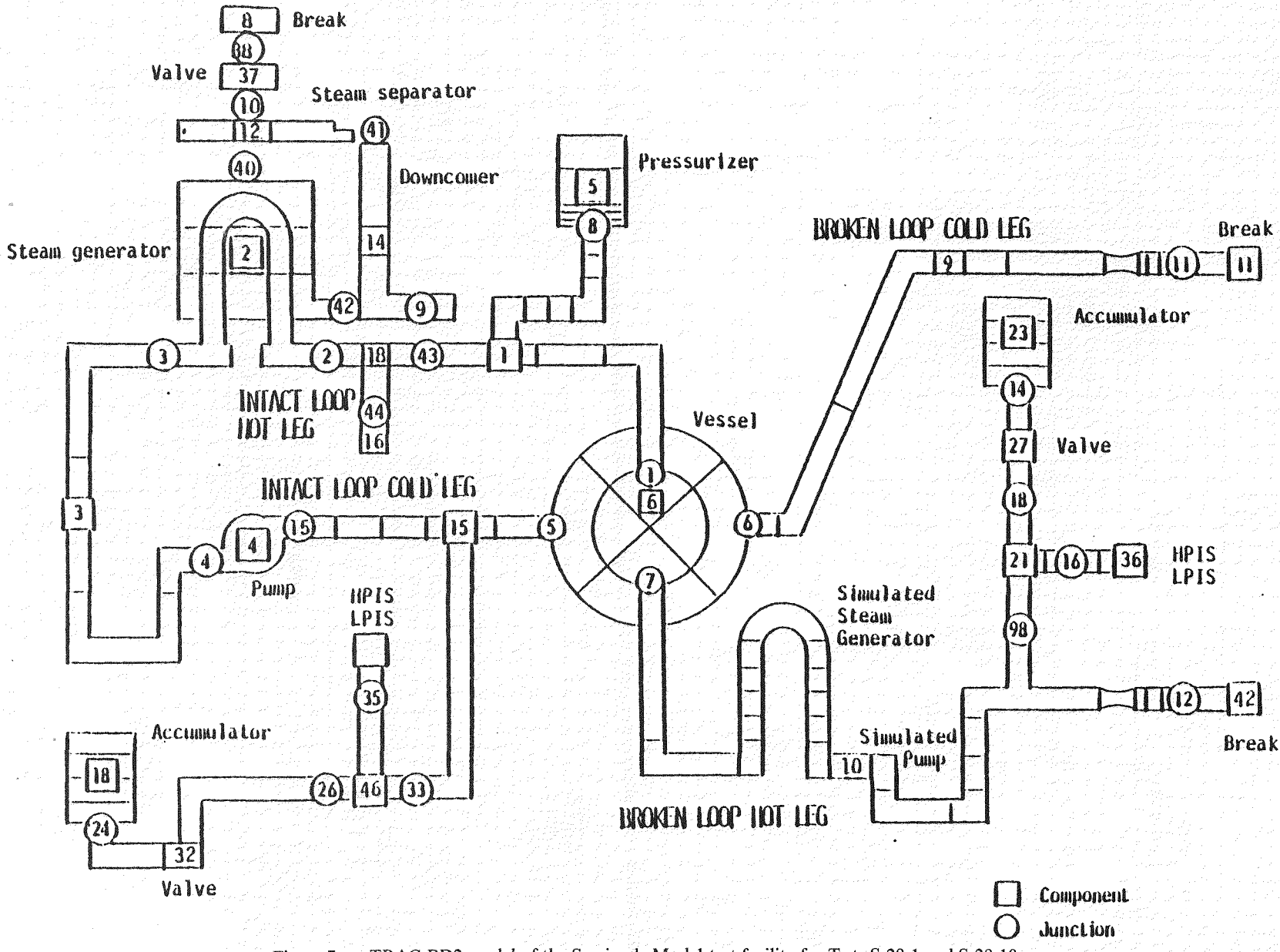

Figure 7. TRAC-PD2 model of the Semiscale Mod-1 test facility for Tests S-28-1 and S-28-10.

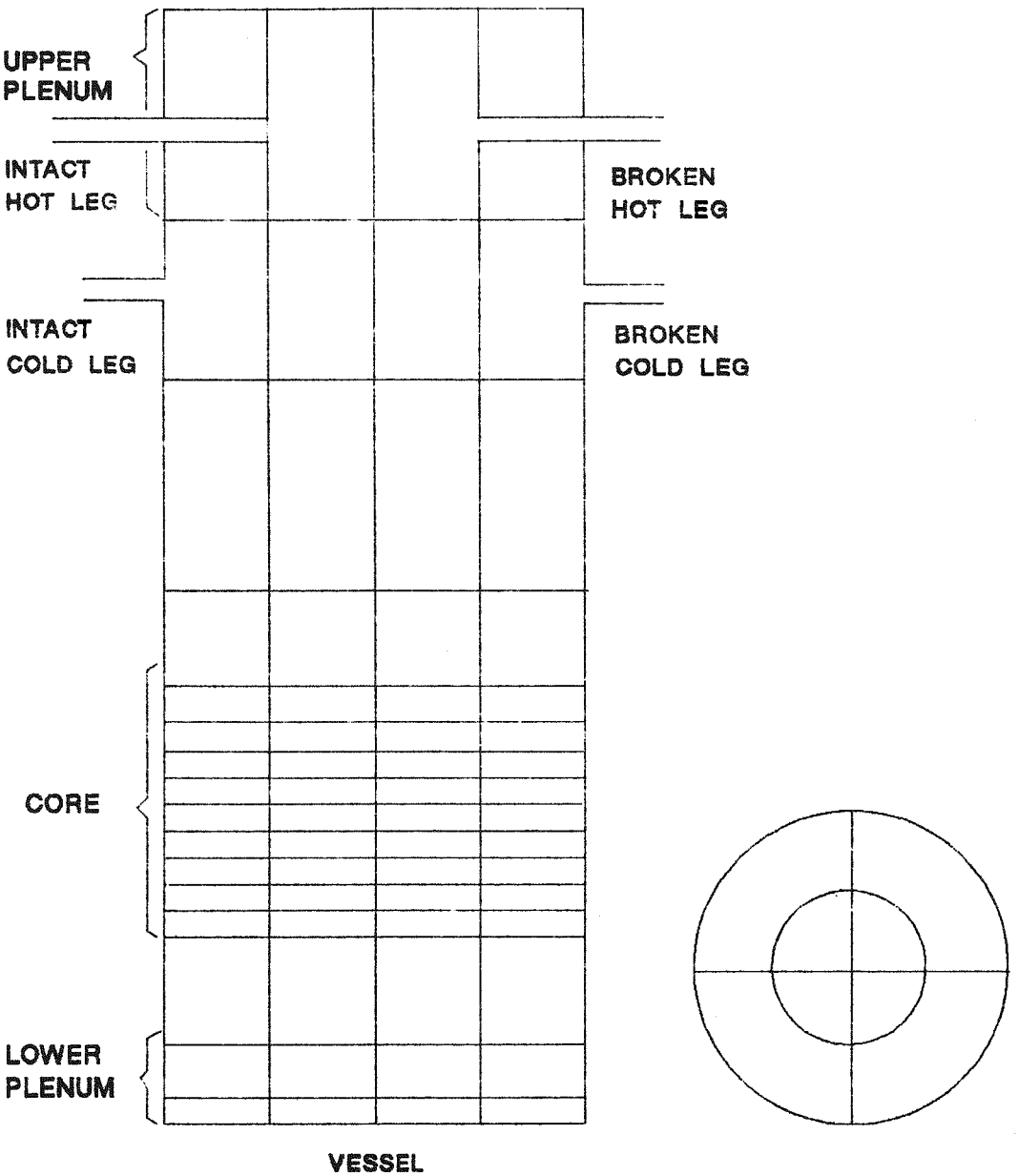

Figure 8. TRAC-PD2 model of the Semiscale Mod-1 vessel for Tests S-28-1 and S-28-10.

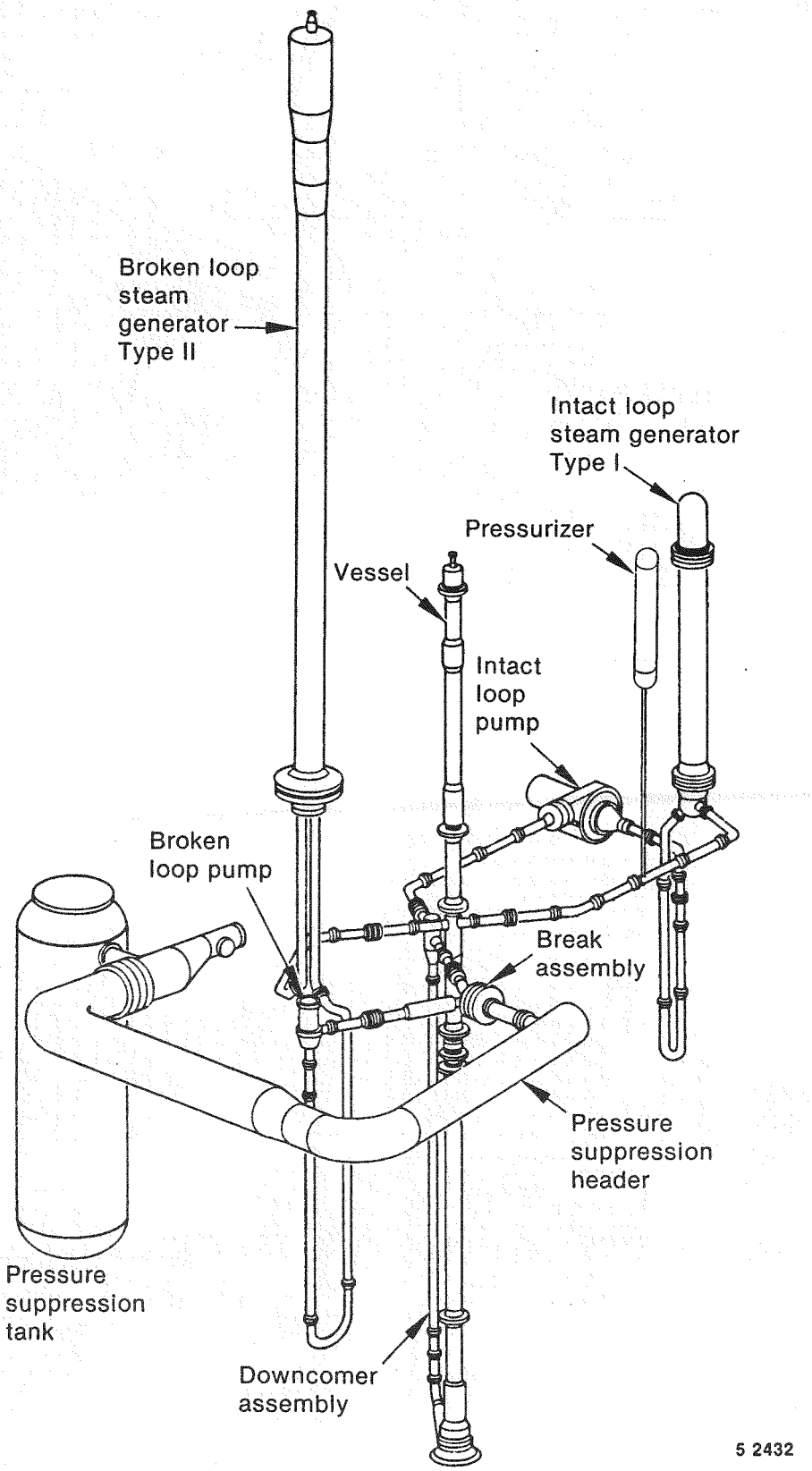

Figure 9. Semiscale Mod-3 test facility.

an external inlet annulus and downcomer pipe. The electrically heated core consisted of 23 3.66-m heater rods.

Nodalization diagrams of the TRAC-PD2 loop and vessel models are shown in Figures 10 and 11, respectively. The model consisted of 25 components. The vessel component was actually a composite model of the vessel, downcomer, and upper head. The vessel component consisted of 19 axial levels divided into two circumferential sections and two concentric rings.

Some modifications to the basic model were required to simulate specific test requirements. Further details regarding the Semiscale Mod-3 TRAC-PD2 models are provided in Appendixes D and E.

2.4 Summary of Test Descriptions and Objectives

The TRAC-PD2 assessment calculations were performed for seven different tests. A brief summary of these tests is provided in this section. More detailed information regarding test objectives and conduct may be found in Appendixes A through E.

2.4.1 PKL Test K5A. The K5A test was performed to simulate a 200% double-ended cold leg break with ECC injection into the intact loop cold legs and downcomer. The test simulated both the refill and reflood portions of the LOCA. The experiment start-up sequence was unique in that all liquid was initially removed from the system and the testing was started with the core and lower plenum filled only with steam.

2.4.2 Semiscale Mod-1 Test S-04-5. The S-04-5 test was performed to simulate a double-ended cold leg break with ECC injection into the intact and broken loop cold legs.

2.4.3 Semiscale Mod-1 Test S-28-1. The S-28-1 test was performed to simulate a double-ended cold leg break, with a subsequent failure of 60 steam generator tubes 40 s after initiation of the LOCA. The calculation predicted the blowdown, refill, reflood, and core quench phenomena during the first 60 s of the test.

2.4.4 Semiscale Mod-1 Test S-28-10. The S-28-10 test was performed to simulate a double-ended cold leg break, with a subsequent failure of 12 steam generator tubes 60 s after initiation of the LOCA. The calculation predicted the blowdown, refill, reflood, and core quench phenomena during the first 120 s of the test.

2.4.5 Semiscale Mod-3 Test S-07-4. The S-07-4 test was performed to study lower plenum injection reflooding at a pressure of 0.414 MPa (60 psia). The test was initiated with the vessel liquid level at the bottom of the heated core. The calculation predicted the first 100 s of the experiment.

2.4.6 Semiscale Mod-3 Test S-SB-2A. The S-SB-2A test was performed to simulate a 2.4% cold leg break in a Westinghouse four-loop PWR in full-power operation. The calculation was performed for the first 1500 s of the test.

2.4.7 Semiscale Mod-3 Test S-SB-4. The S-SB-4 test was performed to simulate a 2.5% cold leg break test that was performed in the LOFT facility at the INEL (Test L3-1). Test S-SB-4 was conducted primarily to identify the effect of LOFT initial conditions and configuration on system behavior during a small-break loss-of-coolant experiment. The difference between this test and Test S-SB-2A was that this break was isolated from the steam generator with an upstream valve. The calculation was performed for the first 1260 s of the test.

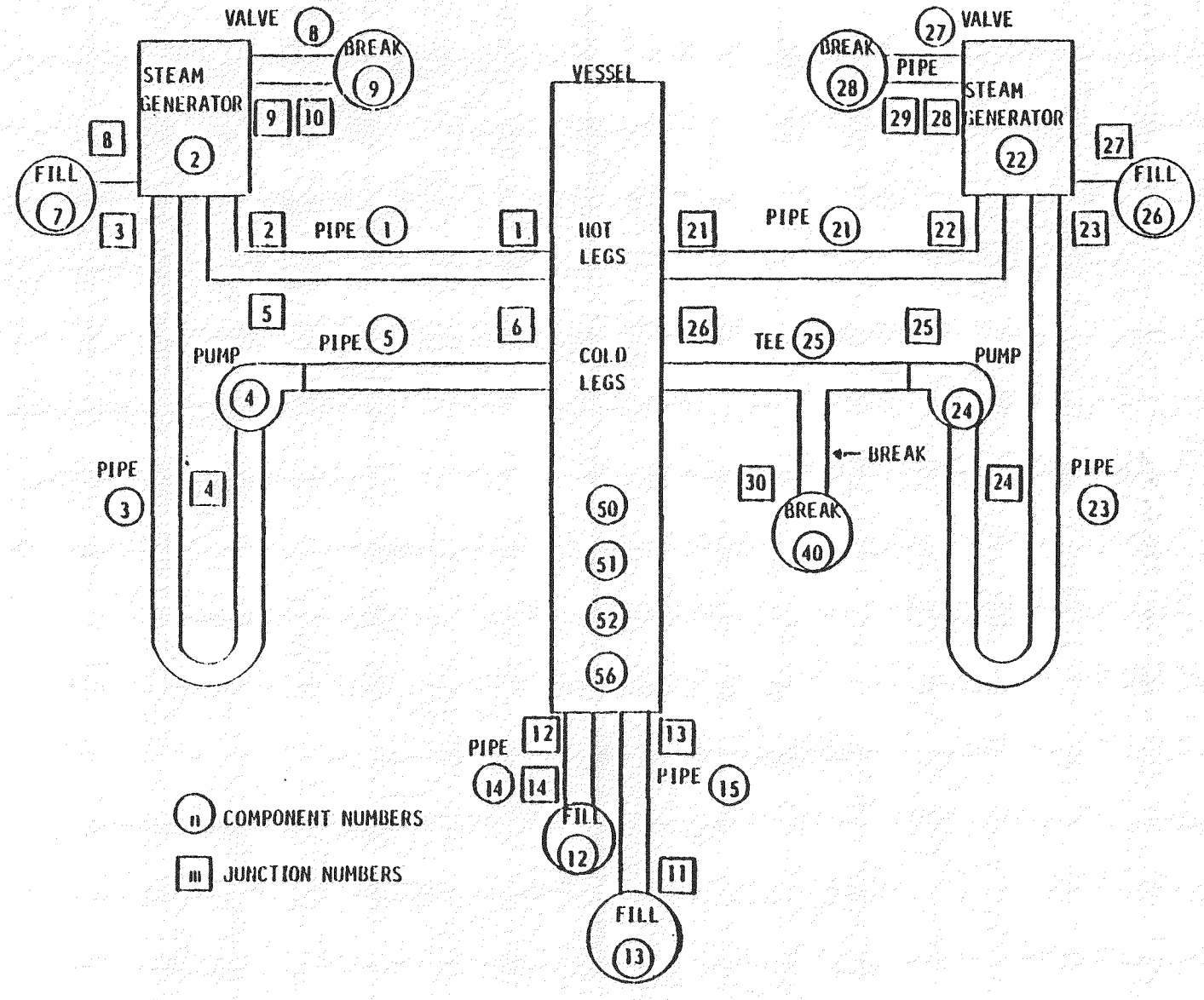

Figure 10. TRAC-PD2 model of the Semiscale Mod-3 test facility.

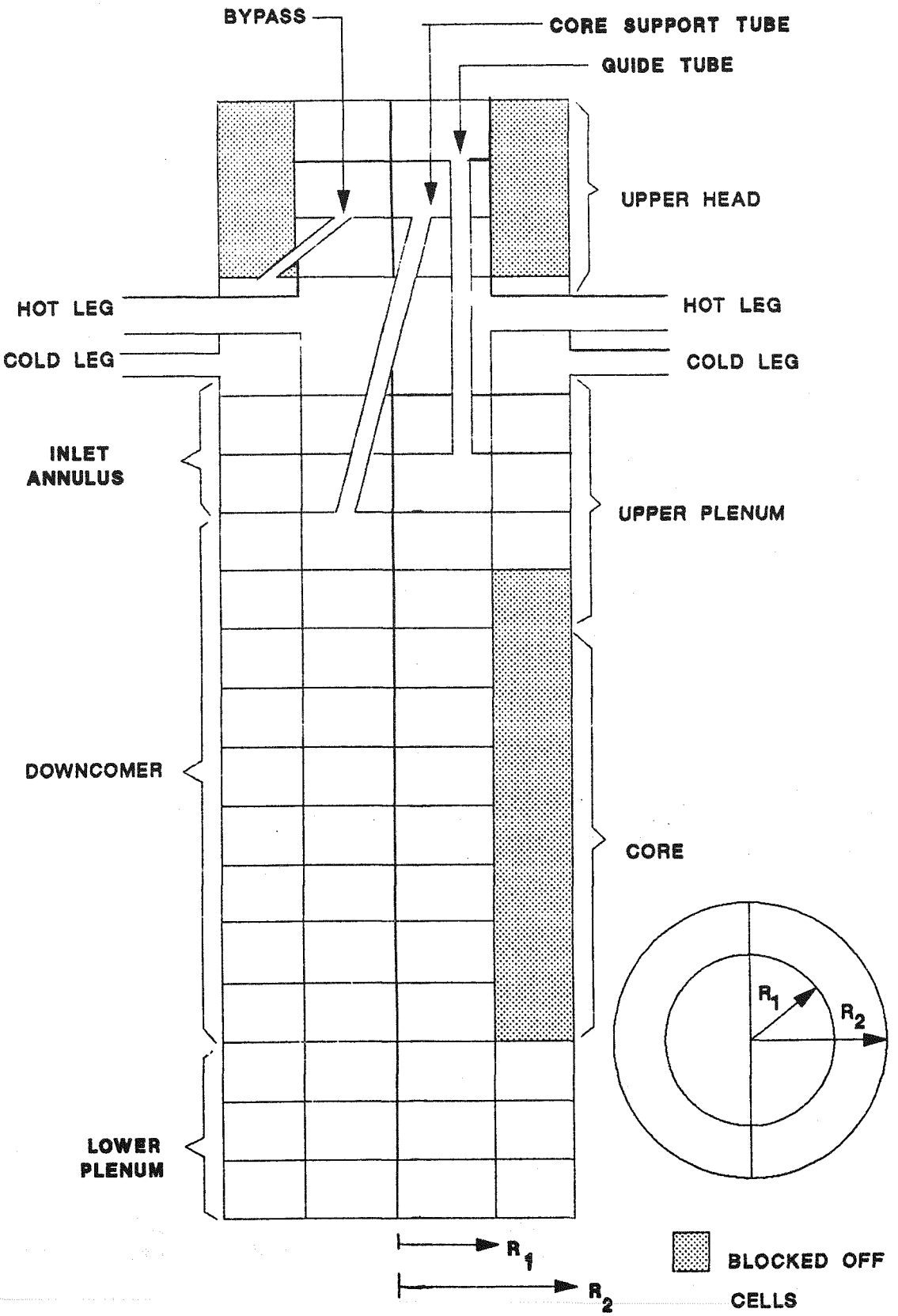

Figure 11. TRAC-PD2 model of the Semiscale Mod-3 vessel.

3. SUMMARY OF CALCULATED RESULTS

Results from the cold leg break assessment calculations are summarized in the following sections. The calculated results are compared to the corresponding test data, and conclusions regarding the adequacy of the TRAC-PD2 code and the models are reviewed.

Calculated and measured break flow results are compared with test data in Section 3.1. Calculated and measured primary coolant system pressure responses are addressed in Section 3.2. Calculated and measured reactor core flow data and ECC data are discussed in Section 3.3. Cladding temperature responses are summarized in Section 3.4. The purpose of these sections is to summarize the results of the various calculations without providing additional analysis regarding comparisons. Greater detail regarding specific results may be obtained from Appendixes A through E.

3.1 Assessment of Break Flow Rate Response

Break flow rate response was addressed in all but the small-break calculations (S-SB-2A and S-SB-4) and the Semiscale reflood test (S-07-4), although break flow rate was briefly discussed in the conclusions of the S-SB-4 section (Appendix E).

The cold leg break flow rate response for the PKL Test K5A calculation is shown in Figure 12. The calculated break flow rate was generally less than the measured flow rate. The relatively large oscillations in the break flow were postulated to be caused by injection of ECC water, which resulted in periods of condensation depressurization followed by periods of repressurization. The measured data in Figure 12 represent the average cold leg mass flow and were obtained by digitizing the raw data. The measured cold leg flow rate also oscillated, but the magnitude of the oscillations was less.

The broken loop cold leg flow rate response for Semiscale Mod-1 Test S-04-5 is shown in Figure 13. The flow rate response agreed reasonably well with the measured data after the initial surge of water out the break.

The broken loop cold leg mass flow rate responses for Semiscale Mod-1 Tests S-28-1 and S-28-10 are shown in Figures 14 and 15, respectively. The calculated break flow rates were less than the measured flow rates during the first 2 s of the calculations, then were greater than measured until 14 s. The differences between the calculated and measured flow rates contributed to inaccuracies in the calculation of the system pressure responses during the first 14 s. After 14 s, the calculated depressurization rates agreed with the data.

The broken loop accumulator model had 33.4 kg of subcooled liquid, whereas the accumulator in the experiment had 16.42 kg of subcooled liquid. Consequently, the test accumulator liquid was depleted during the calculation. This difference did not adversely affect the results of the calculation, because the accumulator liquid was expelled through the break between 40 and 50 s.

Break flow rate response in the Semiscale Mod-3 small-break tests was not addressed in the body of the report, but was mentioned in the conclusions. It was stated that the calculated break flow was probably less than the measured flow rate during the subcooled and transition break flow portions of the calculation, since system mass was determined to be less than the measured amount. Without adequate test data, comparison of calculated and measured data of other system parameters is questionable.

The conclusions regarding break flow response are:

1. TRAC-PD2 break flow calculations were sensitive to model nodalization and were judged to be only adequate for large-break applications.

2. Break flow calculations were very sensitive to initial conditions in the blowdown piping downstream of the break.

3. Consistent calculation of break flow rate response relative to measured data did not occur in the calculations. Calculated break flow was greater than measured in the small-break calculations (by inference from the calculated primary system mass inventory) and was less than measured in the PKL K5A, S-28-1, and S-28-10 calculations.

4. Modeling of the break downstream conditions and nodalization of the break

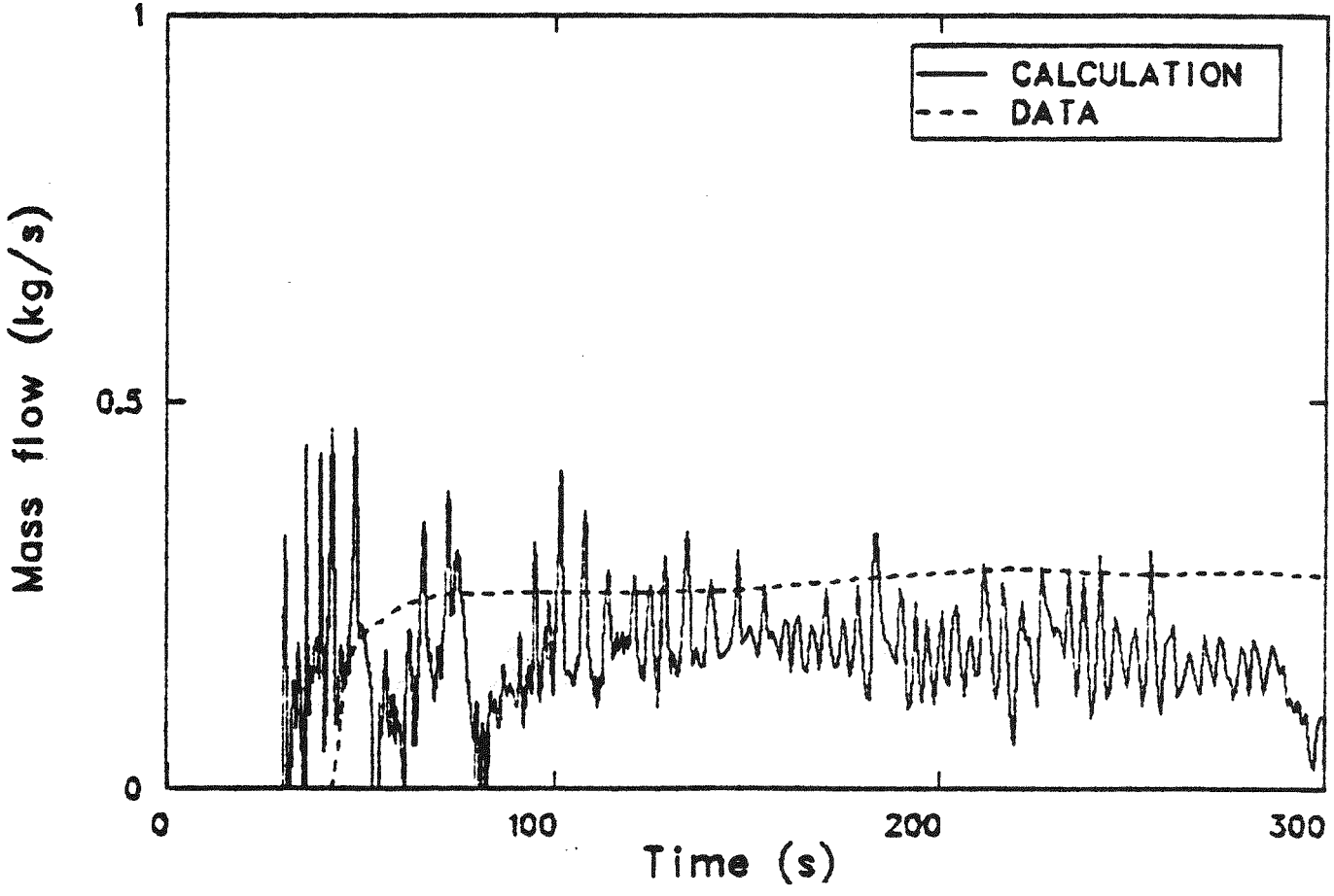

Figure 12. Calculated and measured cold leg break flow response for PKL Test K5A.

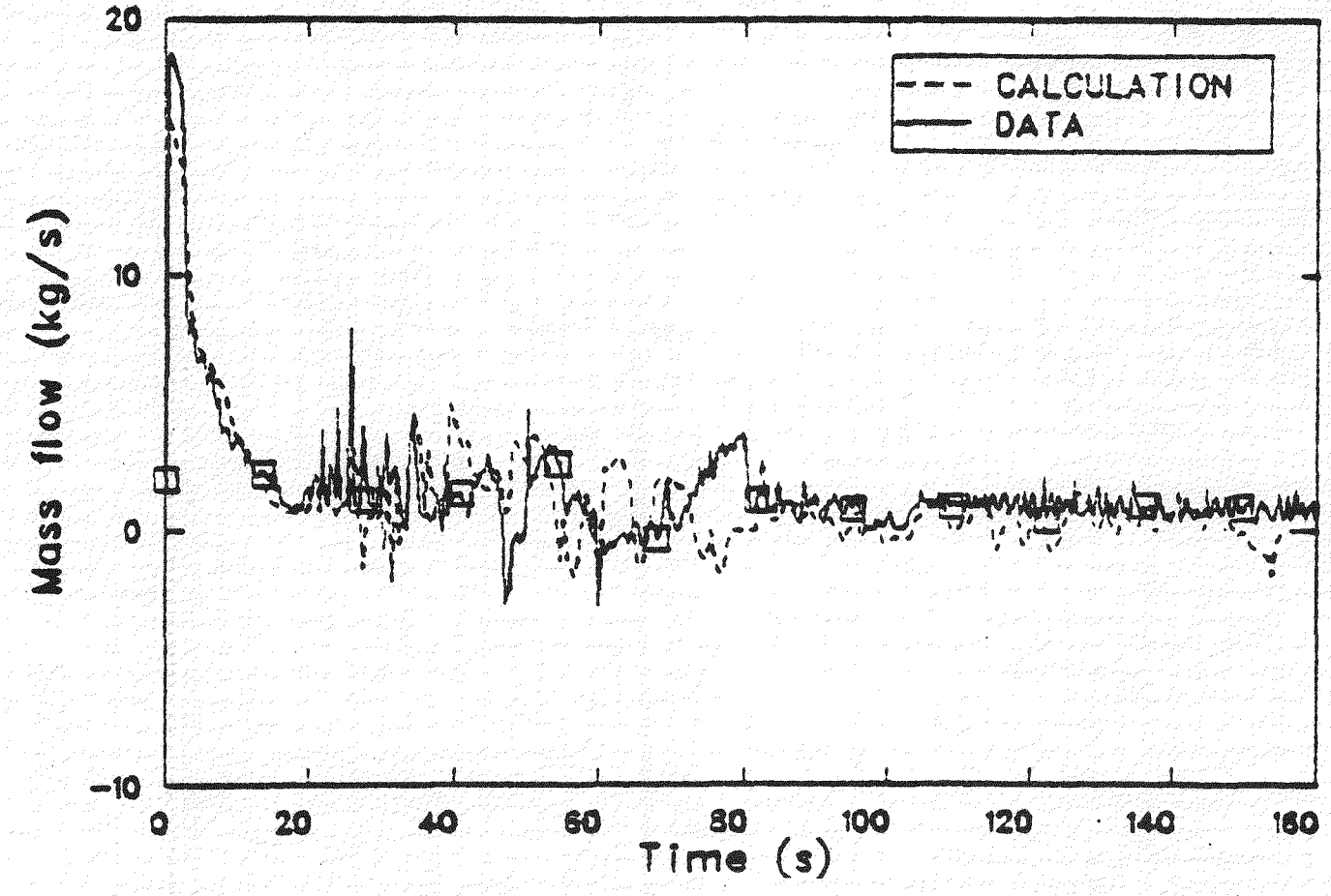

Figure 13. Calculated and measured cold leg break flow response for Semiscale Mod-1 Test S-04-5.

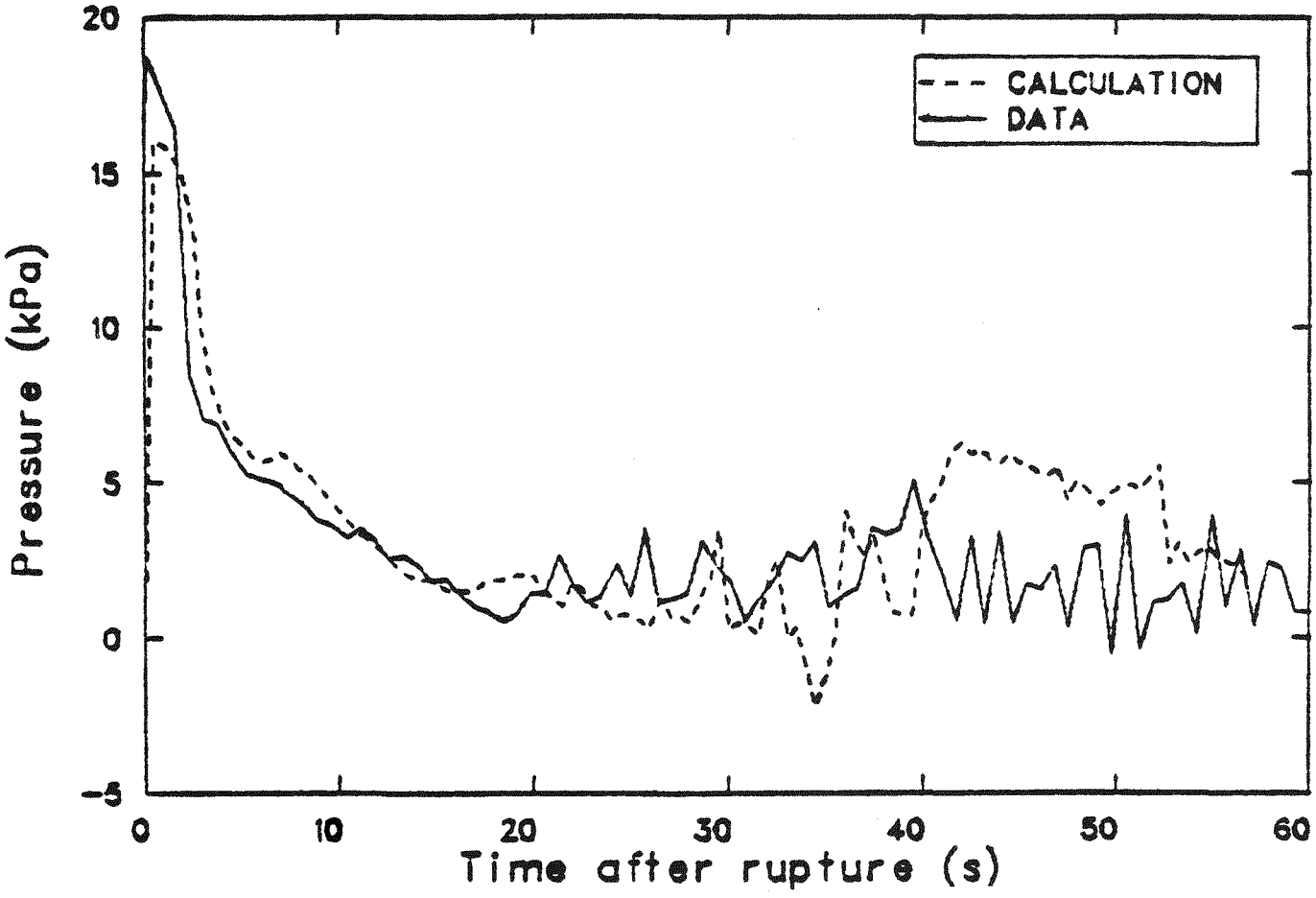

Figure 14. Calculated and measured cold leg break flow response for Semiscale Mod-1 Test S-28-1.

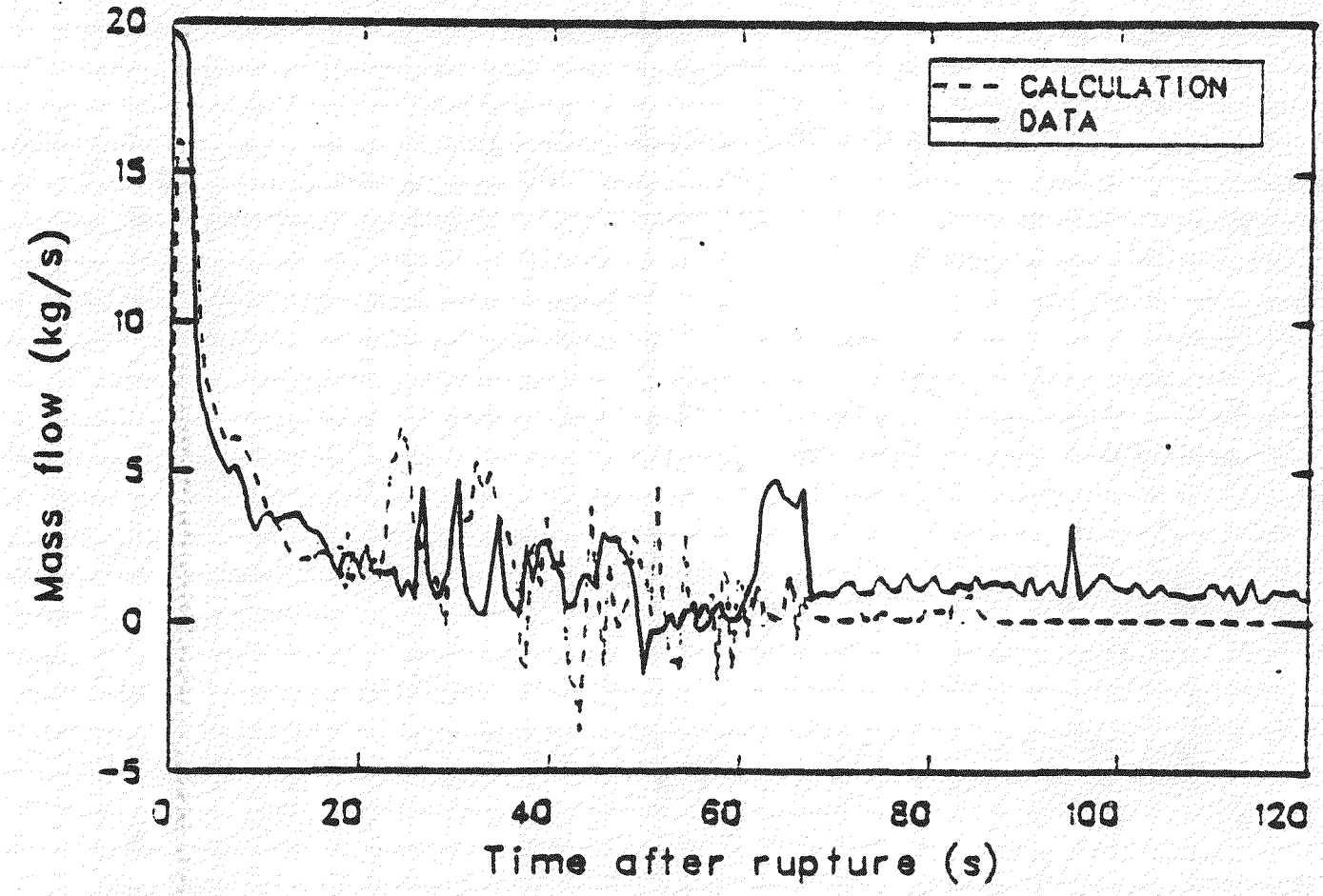

Figure 15. Calculated and measured cold leg break flow response for Semiscale Mod-1 Test S-28-10.

upstream geometry appear to be the most significant factors in accurately calculating the break flow response. A spectrum of break flow calculations can result in the correct break flow response; but the probability for the break may be different. For example, if the calculated break flow for a 3-in. break is the same as the measured flow for a 2-in. break, the probability of failing a 3-in. line versus a 2-in. line must be considered when determining the risk to the public.

3.2 Assessment of Primary System Pressure Response

The measured and calculated primary system pressure responses are discussed in this section. The pressure responses for six of the tests were available. (Semiscale Mod-3 Test S-07-4 pressure data were not presented in Appendix D.)

The primary system pressure response in the PKL Test K5A is shown in Figure 16. The calculated primary system pressure in the vessel upper plenum was greater than the measured pressure during the first 50 s of the test, then less than measured for the remainder of the calculation. The initial difference between the calculated and measured pressures appeared to be caused by excessive vapor generation in the core, while the subsequent pressure calculation error was caused by condensation depressurization effects initiated by the injection of subcooled accumulator fluid.

The primary system pressure response of Semiscale Mod-1 Test S-04-5 is shown in Figure 17. The subcooled depressurization phase was accurately calculated; however, the subsequent calculated rate of depressurization was greater than that measured from 3 to 16 s, because the calculated hot leg volumetric discharge flow rate was less than measured. After 30 s, the measured and calculated pressure responses were in good agreement.

The primary system pressure response data for Semiscale Mod-1 Test S-28-1 are shown in Figure 18. The depressurization rate was affected by the break flow rate response. The calculated rate of depressurization was less than that measured during the first 2 s of the test. Between 2 and 35 s, the calculated break flow rate was too high, thereby resulting in a too high rate of system depressurization. After 35 s, the calculated and measured pressures were in reasonable agreement.

The primary system pressure response data for Semiscale Mod-1 Test S-28-10 are shown in Figure 19. The calculated pressure was too high from about 2 to 10 s, caused by the initial 2 s of calculated break flow rate. The calculated break flow rate from 2 to 14 s resulted in a too high rate of primary system depressurization; consequently, the primary system pressure was too low until 40 s. After 40 s, the calculated pressure response was the same as the measured response. The trends of the measured and calculated pressure data are in good agreement throughout the period of the calculation.

The primary system pressure response data for Semiscale Mod-3 Test S-SB-2A are shown in Figure 20. The subcooled depressurization rate was adequately calculated by TRAC-PD2; however, the calculated break flow rate was too low during the period of break flow transition, i.e., the period when break quality is between 2% and 100%. Consequently, the rate of primary system depressurization was too high between 50 and 200 s. TRAC-PD2 calculated that the broken loop pump seal would clear at 300 s and the core would start to uncover at 310 s. The combined effect of these two events was a calculated rate of depressurization that was too high, culminating in a calculated time of accumulator injection initiation that was too early. The injection of the accumulator fluid at 600 s ultimately resulted in a repressurization of the primary system caused by increased vapor generation in the core as the vessel refilled. The calculated rate of primary system depressurization after 600 s was higher than measured because of the condensation depressurization effects that were calculated by TRAC-PD2.

The primary system pressure response data for Semiscale Mod-3 Test S-SB-4 are shown in Figure 21. The subcooled depressurization rate was adequately calculated; however, as in the S-SB-2A calculation, the subsequent pressure response was not as well represented. The broken loop pump seal was calculated to clear at 200 s, which resulted in a predicted calculated response similar to that of S-SB-2A.

A summary of the calculated and measured times of accumulator injection is presented in Table 2.

The conclusions regarding primary system pressure response are:

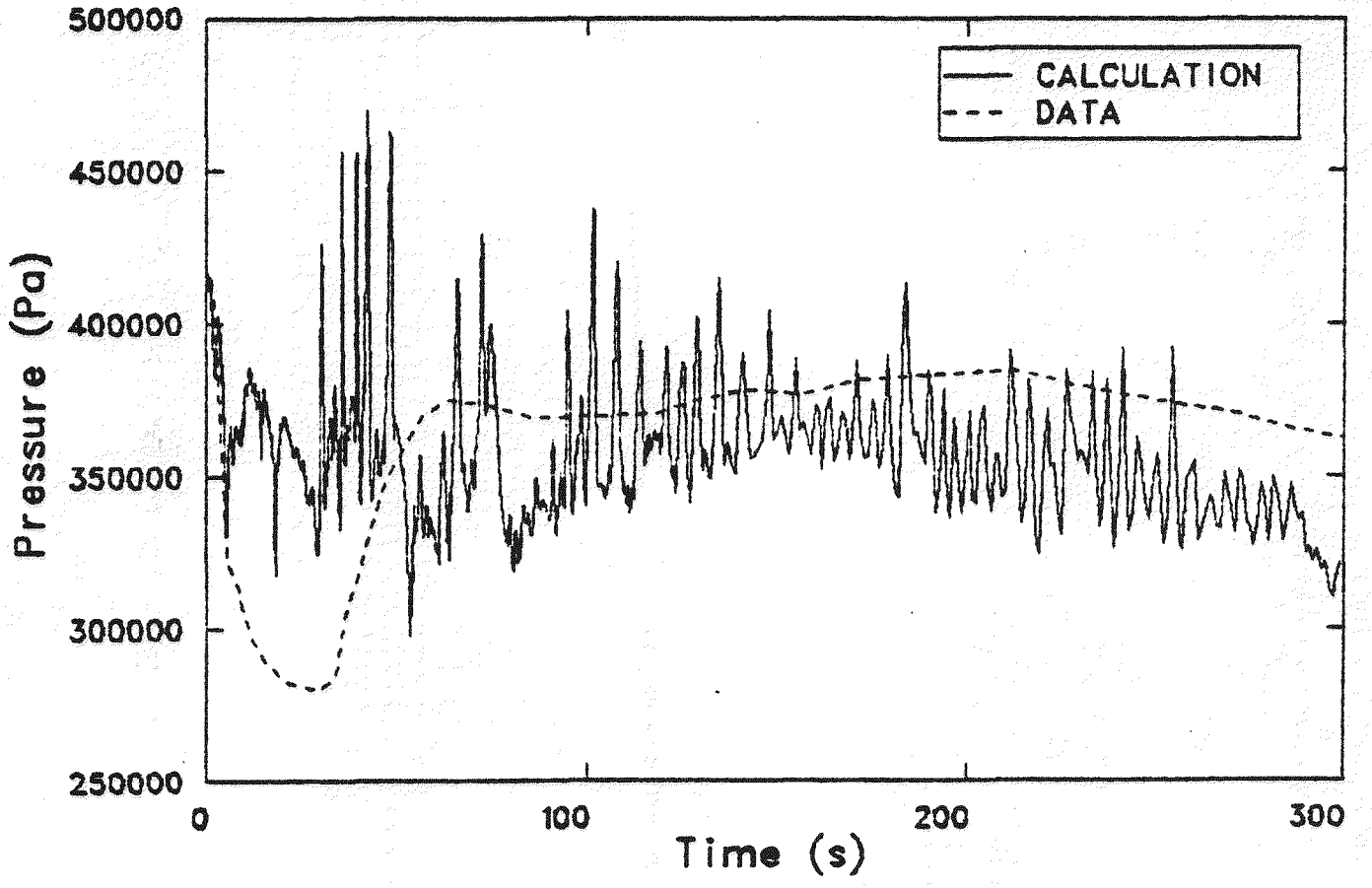

Figure 16. Calculated and measured upper plenum pressure response for PKL Test K5A.

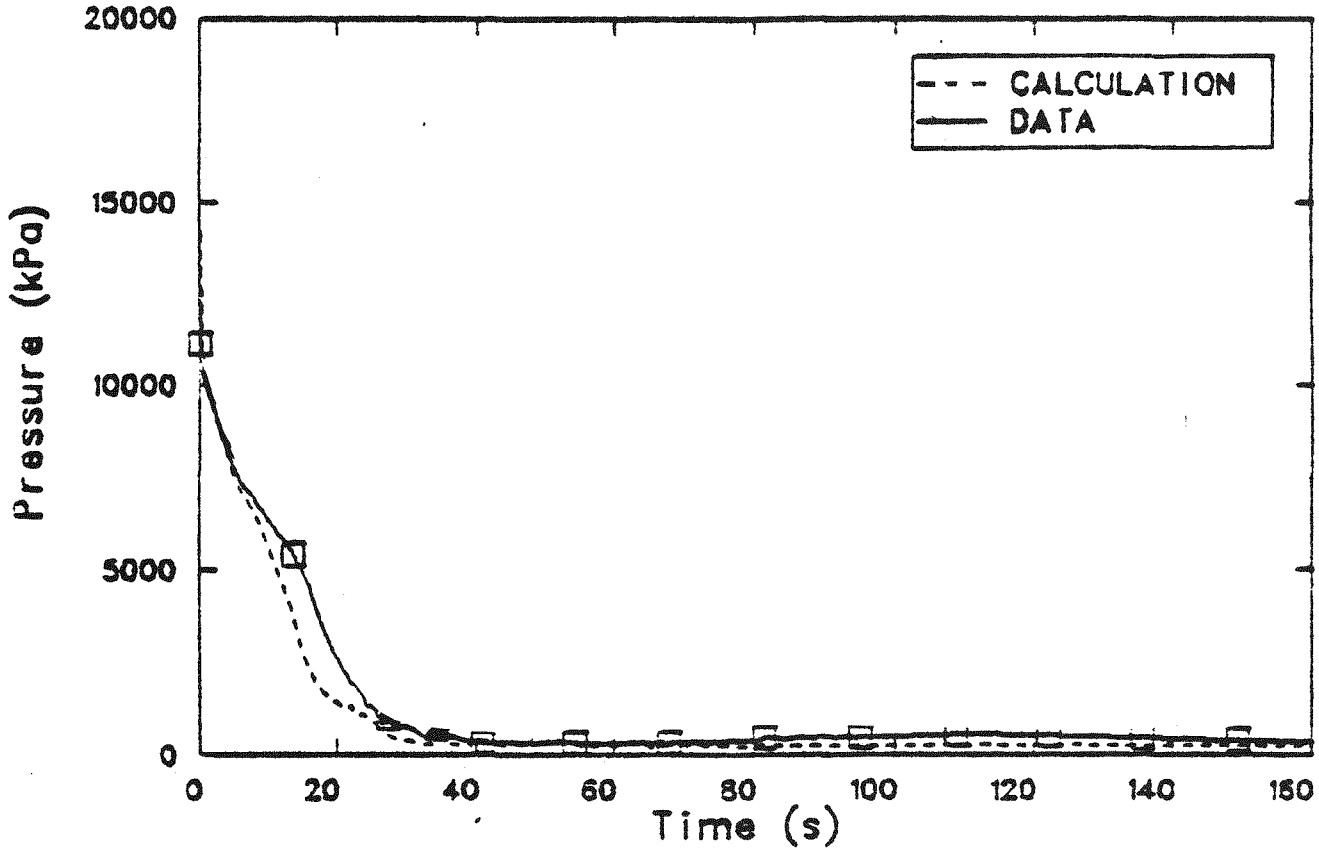

Figure 17. Calculated and measured upper plenum pressure response for Semiscale Mod-1 Test S-04-5.

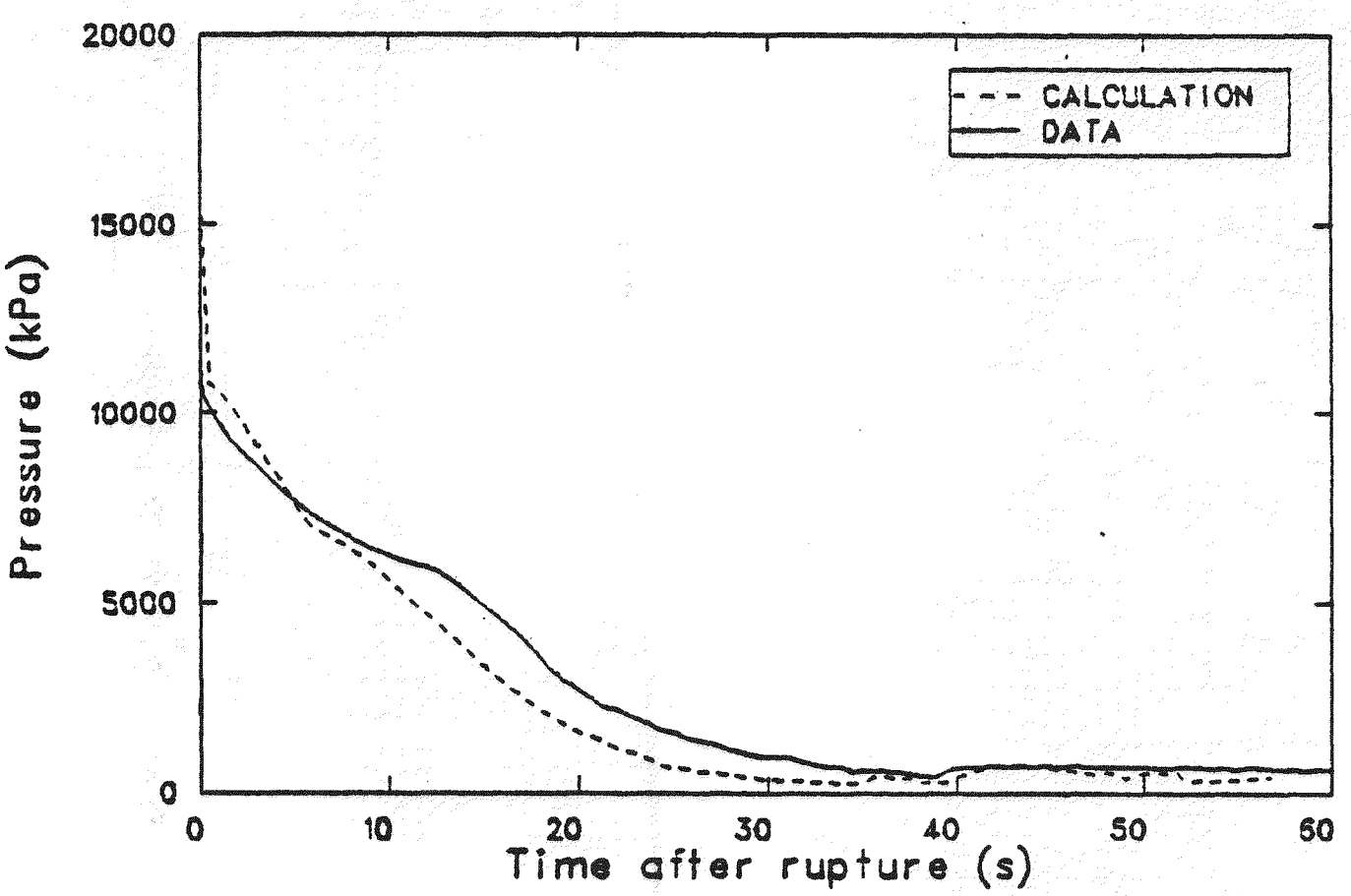

Figure 18. Calculated and measured system pressure response for Semiscale Mod-1 Test S-28-1.

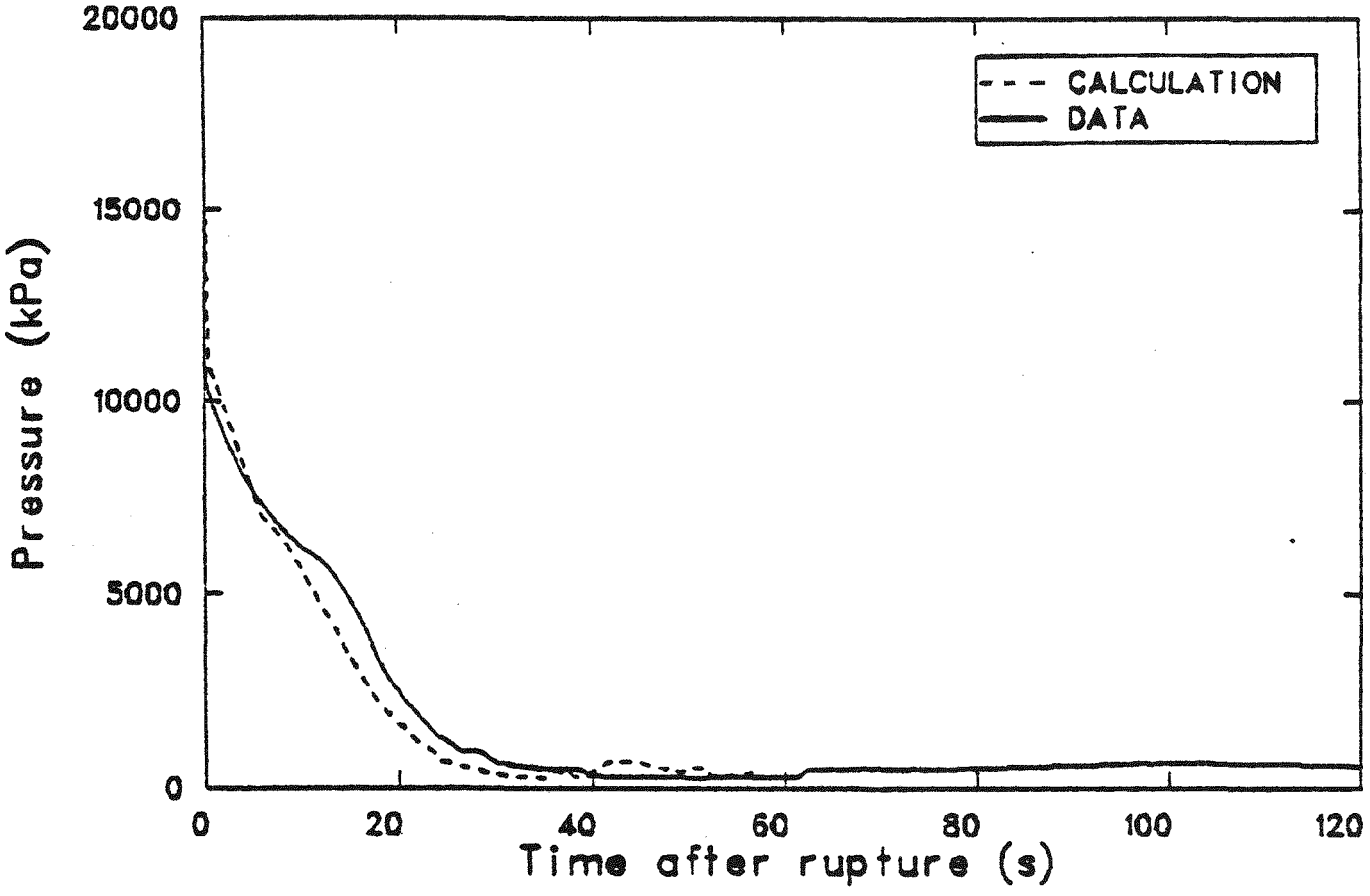

Figure 19. Calculated and measured system pressure response for Semiscale Mod-1 Test S-28-10.

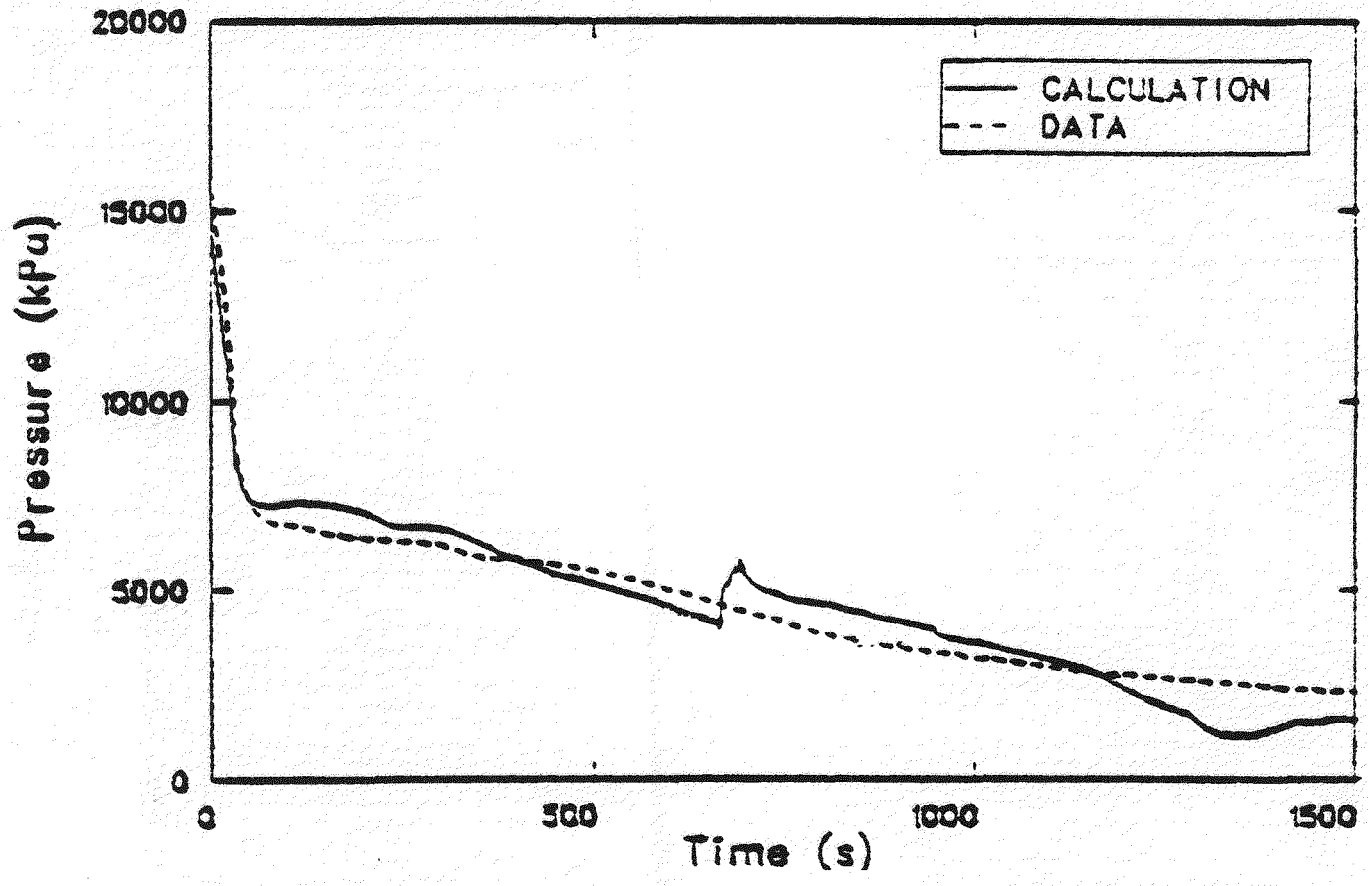

Figure 20. Calculated and measured upper plenum pressure response for Semiscale Mod-3 Test S-SB-2A.

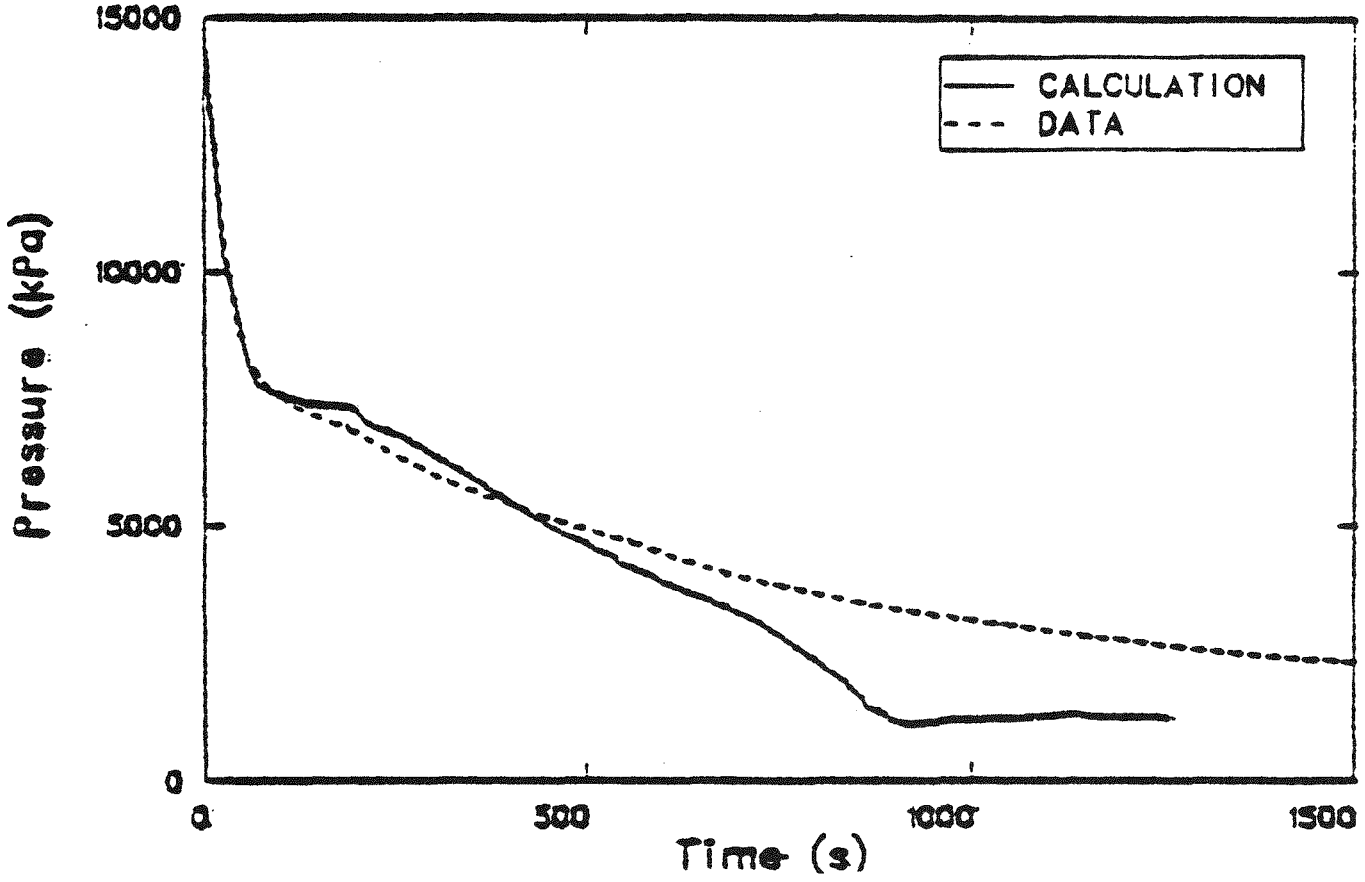

Figure 21. Calculated and measured upper plenum pressure response for Semiscale Mod-3 Test S-SB-4.

Table 2. Calculated and measured times of accumulator injection

Test	Calculated (s)	Measured (s)	Difference (s)
S-04-5			
Broken	3	3.5	-0.5
Intact	16	16.5	-0.5
S-28-1			
Broken	3	1	2
Intact	13	17	-4
S-28-10			
Broken	1	2	-1
Intact	13	16	-3
S-SB-2A			
Broken	600	790	-190
Intact	595	740	-145
S-SB-4			
Broken	480	550	-70
Intact	480	550	-70

1. Inaccurate modeling of the break geometry (incorrect friction factors, inadequate nodalization, and failure to specify a reasonable set of discharge coefficients) caused inaccuracies in the calculation of break flow rate and, consequently, the rate of primary system depressurization.

2. Mass distribution in the primary coolant loops influenced the time of accumulator injection initiation and, consequently, the primary system pressure response.

3. The subcooled depressurization phase is adequately represented by TRAC-PD2.

4. The general trend in the calculated predicted pressure response data is reasonably specified by TRAC-PD2 during the saturated blowdown phase.

5. Primary system pressure response was most significantly affected by the break flow rate response and calculation of condensation depressurization that was higher than indicated in the tests.

3.3 Assessment of Core Flow Rate Response

The calculated core flow rate responses are discussed in this section. The core flow response was not addressed in PKL Test K5A (Appendix A).

The core flow behavior for Semiscale Mod-1 Test S-04-5 is shown in Figure 22. The calculated core inlet mass flow rate during the first 4 s was less than that measured. The delay in the lower plenum refill was significantly less in the calculation, because hot wall delay effects in the downcomer were not accurately calculated. This could have been caused by a modeling error in specifying the effective thickness of the lumped parameter downcomer wall heat structure. The oscillatory inlet flow rates shown in Figure 22 did not occur in the test. The calculated time of fuel rod quench indicates that TRAC-PD2 apparently did not correctly calculate the amount of liquid entrainment into the core.

The calculated core inlet mass flow rate response for Semiscale Mod-1 Test S-28-1 is compared to the

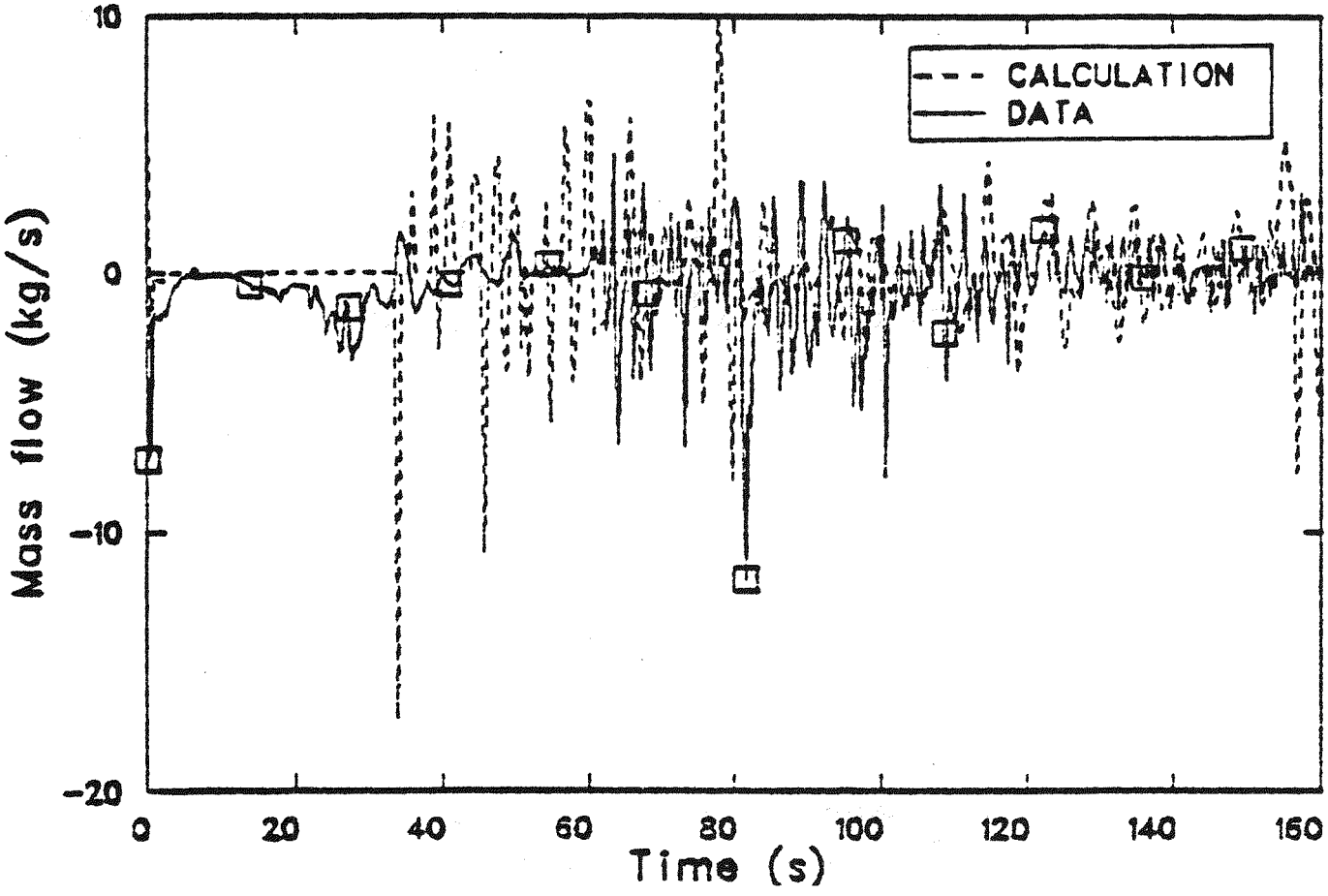

Figure 22. Calculated and measured core inlet flow rate response for Semiscale Mod-1 Test S-04-5.

measured data in Figure 23. The overall response was calculated reasonably well with the exception of the flow oscillations between 38 and 42 s. These oscillations were caused by a combination of rapid vapor generation at the core inlet, alternating with condensation of the vapor at the top of the downcomer. The vapor generation was caused when the core began reflooding, forcing liquid back out of the core and into the downcomer. As the downcomer level increased, vapor in the top of the downcomer mixed with the cold leg liquid, thereby causing the vapor to condense. This increased the reversed flows at the core inlet. As the liquid level in the downcomer increased, the resulting density head increase overcame the reversed flow and resulted in a resumption of a positive flow at the core inlet.

The calculated core inlet mass flow rate response for Semiscale Mod-1 Test S-28-10 is compared to the measured data in Figure 24. The core flow rate response was reasonably well calculated for the first 30 s. Between 30 and 55 s, the flow oscillations were too high. This was caused by the initiation of reflood at 35 s, as opposed to the 55-s reflood initiation in the test. A second factor was a too high rate of accumulator flow. The calculated overall core inlet flow response was in general agreement with the measured data.

The calculated core inlet mass flow rate response for Semiscale Mod-3 Test S-07-4 is compared to the measured data in Figure 25. The core flow rate response was not accurately calculated by TRAC-PD2. Large manometer-type oscillations of flow between the core and the downcomer were calculated. These oscillations were caused by excessive condensation depressurization in the upper downcomer coupled with repressurization caused by steam generation in the upper core as the core refilled. These oscillations appeared to be a significant factor in the break flow rate response and the primary system pressure response.

The calculated core inlet mass flow rate response for Semiscale Mod-3 Test S-SB-2A is inferred by the collapsed level data in Figure 26. The calculated collapsed liquid level in the core agreed with the measured response for the first 300 s, indicating good correspondence between the measured and calculated core flow rate responses. The core level was too low after 300 s, because the test loop seal cleared and the loop seal liquid was forced into the downcomer and vessel. In the calculation, the loop seal water was lost though the break instead of being retained in the system. The calculated rapid increase in the core level at 480 s was caused by accumulator injection. An increase in the calculated accumulator flow rate at 830 s resulted in the core level increasing rapidly to the top of the core, where it remained for the remainder of the calculation. The measured core level indicated a gradual increase after 550 s caused by the accumulator injection.

The calculated core inlet mass flow rate response for Semiscale Mod-3 Test S-SB-4 is inferred by the collapsed level data in Figure 27. A response similar to that calculated for Semiscale Test S-SB-2A is indicated.

The conclusions regarding core flow response are:

1. Condensation depressurization in the top of the downcomer coupled with high rates of vapor generation in the core caused flow oscillations at the core inlet. This behavior was also indicated by the measured data. The initiation of this behavior is dependent on the timing of core reflood, which is dependent in turn on the time of accumulator injection.

2. Downcomer hot wall delay effects were calculated by TRAC-PD2, but the timing of this phenomenon was not accurately calculated. The downcomer wall was modeled as a lumped parameter heat structure, which required the modeler to accurately specify the effective wall thickness. An incorrect specification of the effective wall thickness could have been responsible for the timing of the hot wall delay effects seen in the calculations.

3. Calculation of coolant mass distribution during S-SB-2A significantly affected the results. The calculated mass in the broken loop pump seal was not retained in the system as it should have been, which affected the core flow response. The problem of calculating the correct mass distribution indicates that TRAC-PD2 should not be used for SBLOCA calculations, because incorrectly calculated system mass distribution affects core temperature response.

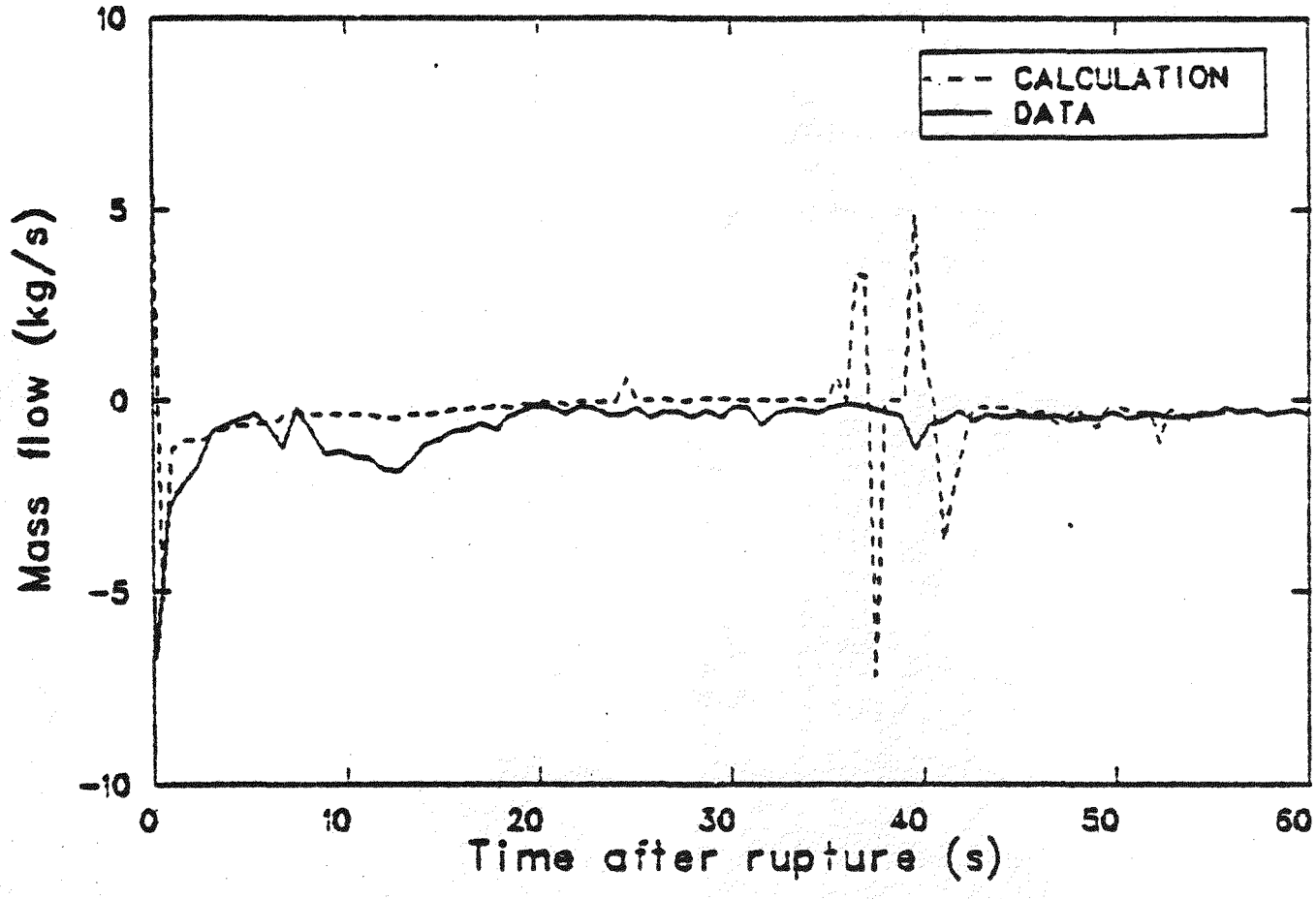

Figure 23. Calculated and measured core inlet flow rate response for Semiscale Mod-1 Test S-28-1.

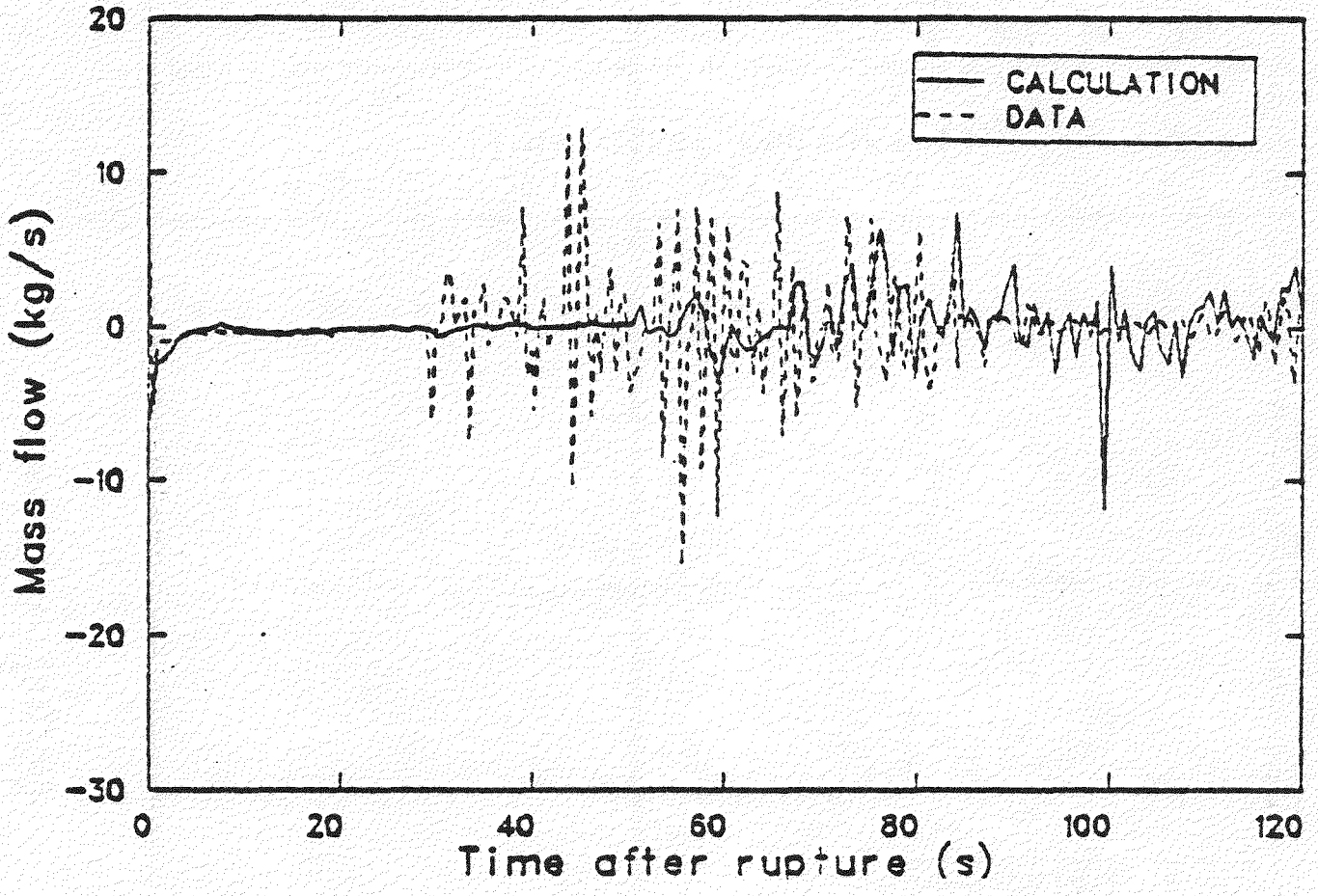

Figure 24. Calculated and measured core inlet flow rate response for Semiscale Mod-1 Test S-28-10.

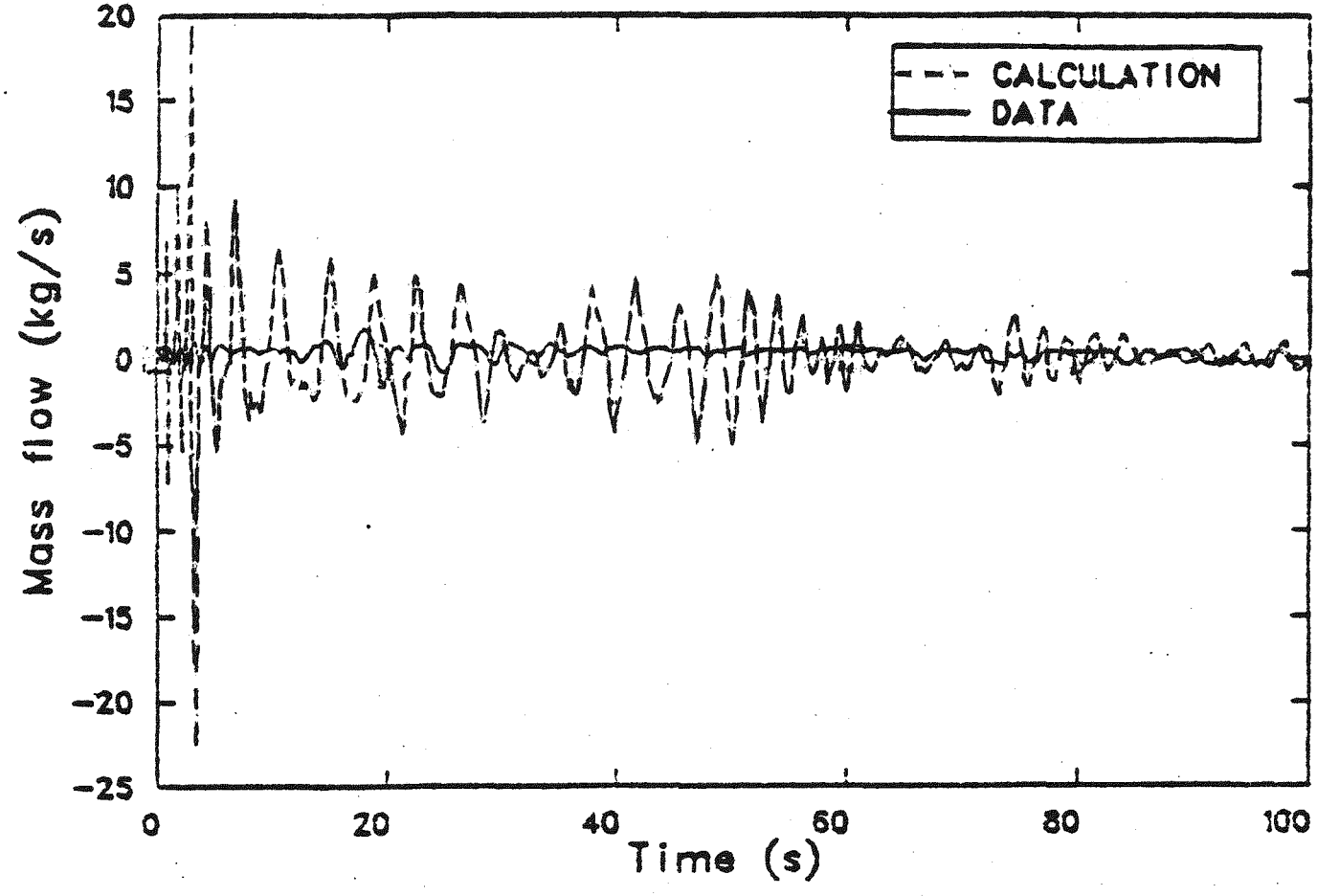

Figure 25. Calculated and measured core inlet flow rate response for Semiscale Mod-3 Test S-07-4.

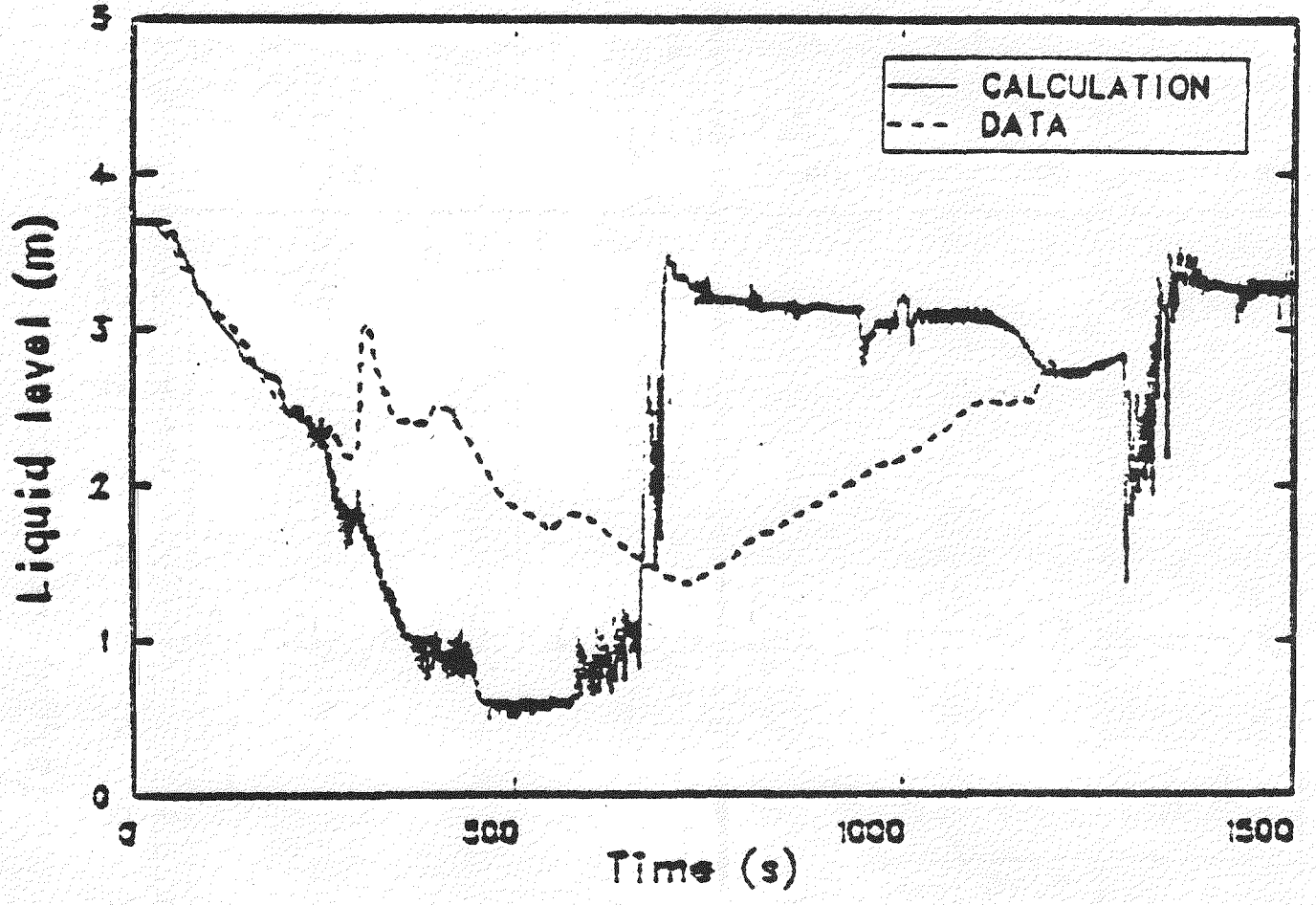

Figure 26. Calculated and measured collapsed core liquid level response for Semiscale Mod-3 Test S-SB-2A.

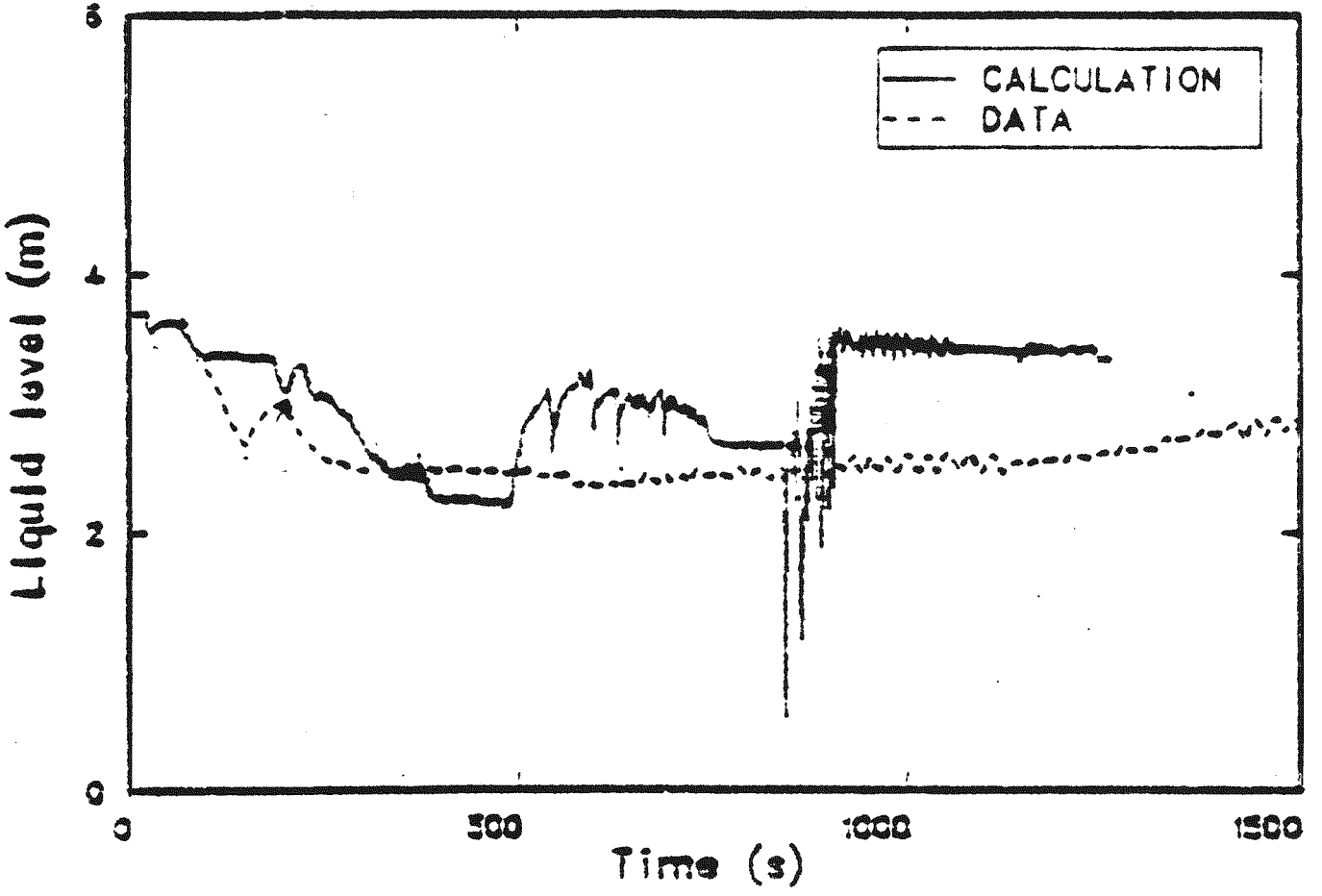

Figure 27. Calculated and measured collapsed core liquid level response for Semiscale Mod-3 Test S-SB-4.

4. Core flow response was generally accurate; however, some inadequacies regarding liquid entrainment were calculated. The significant differences in break flow response caused some problems regarding ECC injection timing.

3.4 Assessment of Cladding Temperature Response

The data obtained from four cladding surface thermocouples in the high-power region of the PKL Test K5A hot channel and the calculated cladding temperature response are shown in Figure 28. The initial cladding temperature increase from 0 to 35 s was calculated very well, as was the peak cladding temperature. The rate of cladding temperature decrease after the peak temperature was reached was higher in the calculation than in the test. Excessive liquid entrainment in the calculation resulted in high heat transfer coefficients, which allowed the cladding to cool faster. The rod quench time was within the scatter of the data; but the accurate calculation of quench time was not considered a fair indicator of the calculation accuracy, because the calculated cladding temperature at the time of quench was lower than the measured values.

The measured and calculated cladding temperature responses in the lower and upper regions of the core for Semiscale Test S-04-5 are shown in Figures 29 and 30; and the times of CHF, PCT, and quench are provided in Table 3. The time of CHF was adequately calculated in the lower regions of the core, but was not accurately calculated in the upper regions. The calculated cladding temperatures were less than the measured temperatures in both the upper and lower regions of the core after 30 s. This was apparently caused by either excessive liquid entrainment in the calculation, higher-than-actual heat transfer coefficients, early initiation of reflood, or a combination of all three. The excessive liquid entrainment could have been responsible for higher-than-actual heat transfer coefficients; higher-than-actual heat transfer coefficients would have been responsible for early initiation of cladding quench. Reflood was initiated earlier in the calculation than in the test, resulting in cladding temperatures that were lower than the measured values after cladding quench.

The calculated cladding temperature responses in the upper half of the core were similar to the measured responses for the first 30 to 36 s of the transient. After 140 s, the calculated heat transfer regime was transition film boiling, indicating the presence of entrained liquid, which resulted in heat transfer coefficients that were too high and earlier calculated times of cladding quench.

The measured and calculated cladding temperature responses in the lower, middle, and upper regions of the core for Semiscale Test S-28-1 are shown in Figures 31 through 33; and a summary of the calculated and measured maximum temperatures in the core is provided in Table 4. The cladding temperature responses were generally well calculated in the lower and middle regions of the core where the CHF phenomenon was correctly calculated to either occur or not occur. CHF was not calculated in the upper region of the core, and the cladding temperatures were consequently too low prior to quench and too high after cladding quench was indicated. The calculated rate of downward quench and the time of quench initiation were less than the measured values caused by the calculation of excessive liquid flashing, which resulted in less liquid inventory available for cladding quench.

The measured and calculated cladding temperature responses in the lower, middle, and upper regions of the core for the Semiscale Test S-28-10 are shown in Figures 34 through 36; and a summary of calculated and measured maximum temperatures in the core is provided in Table 5. The cladding temperature responses were generally best calculated in the lower and middle regions of the core where the CHF phenomenon was correctly calculated to either occur or not occur. The time of core reflood was too early by 20 s and the rate of core injection was too high, resulting in the quench times being too early. The calculated temperature response in the upper portion of the core was not representative of the test data after 30 s, caused by a calculated rewetting of the cladding that was not measured.

The measured and calculated cladding temperature responses in the lower, middle, and upper regions of the core for Semiscale Test S-07-4 are shown in Figures 37 through 39. In the lower elevations, the cladding temperatures were too high by 35 K. This could have been caused by a calculation of insufficient subcooling in the lower portion of the core, which was probably caused by the calculated manometer-type oscillations between the downcomer and core.

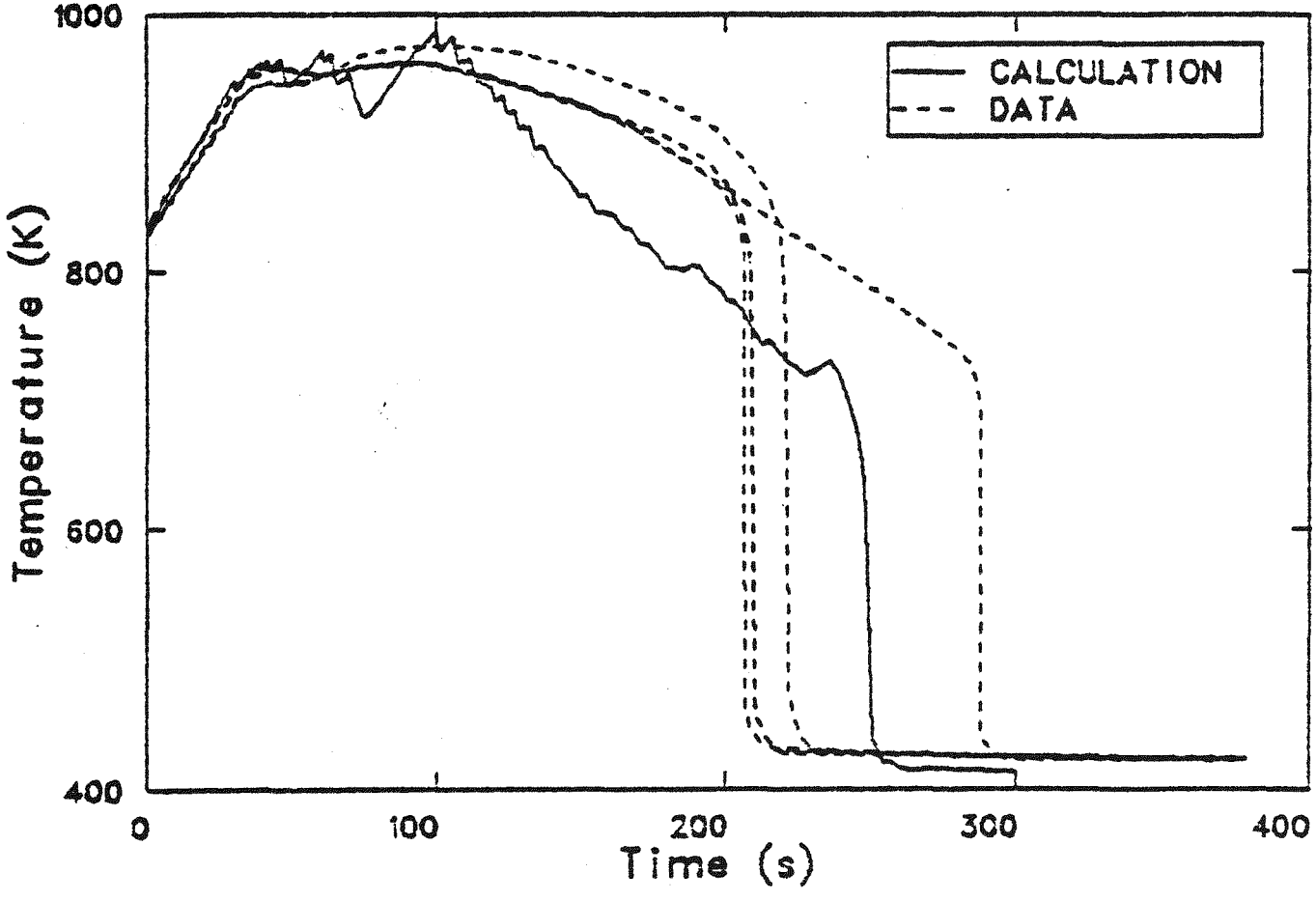

Figure 28. Calculated and measured cladding surface temperature response in the core high power region for PKL Test K5A.

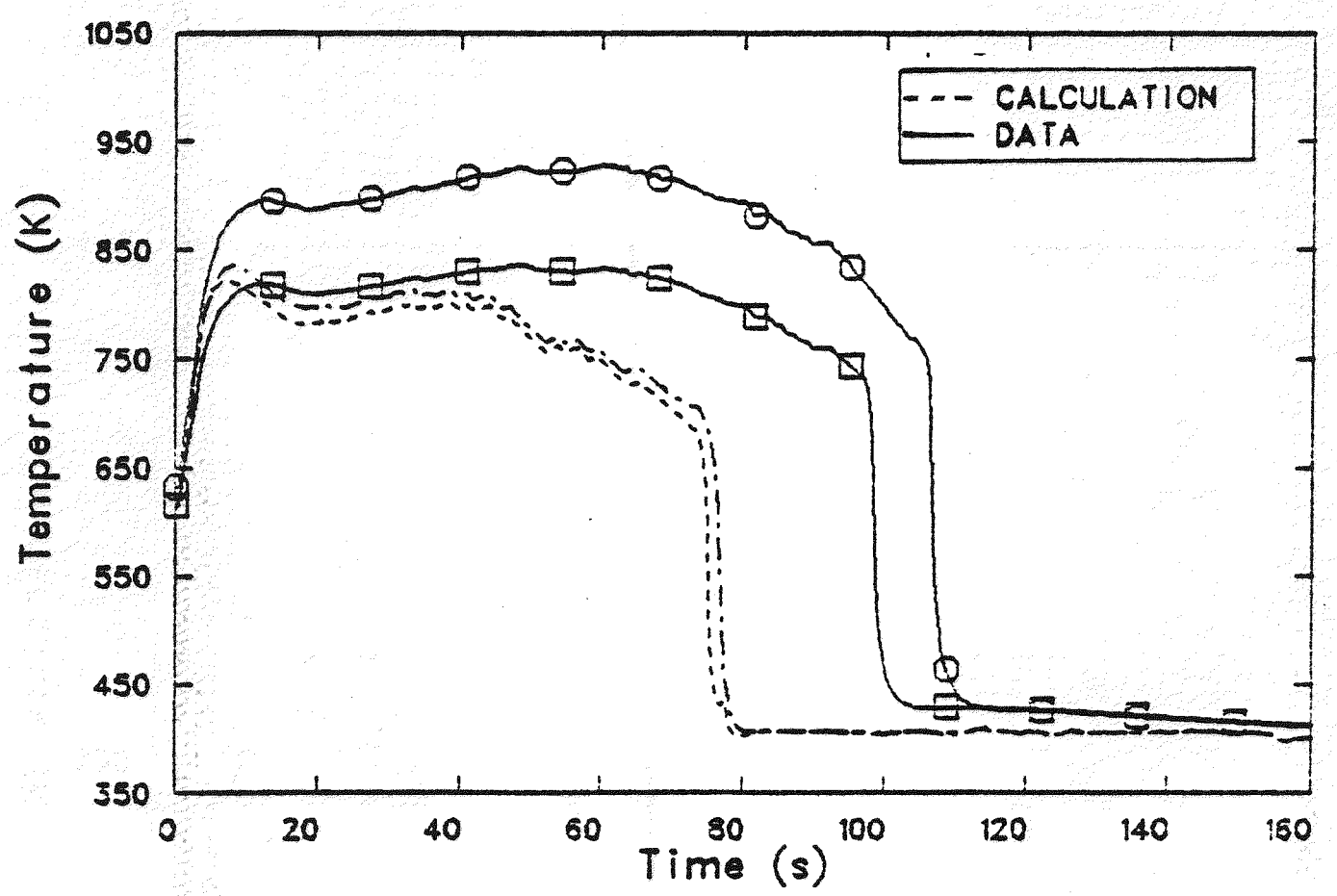

Figure 29. Calculated and measured cladding surface temperature response in the core lower region for Semiscale Mod-1 Test S-04-5.

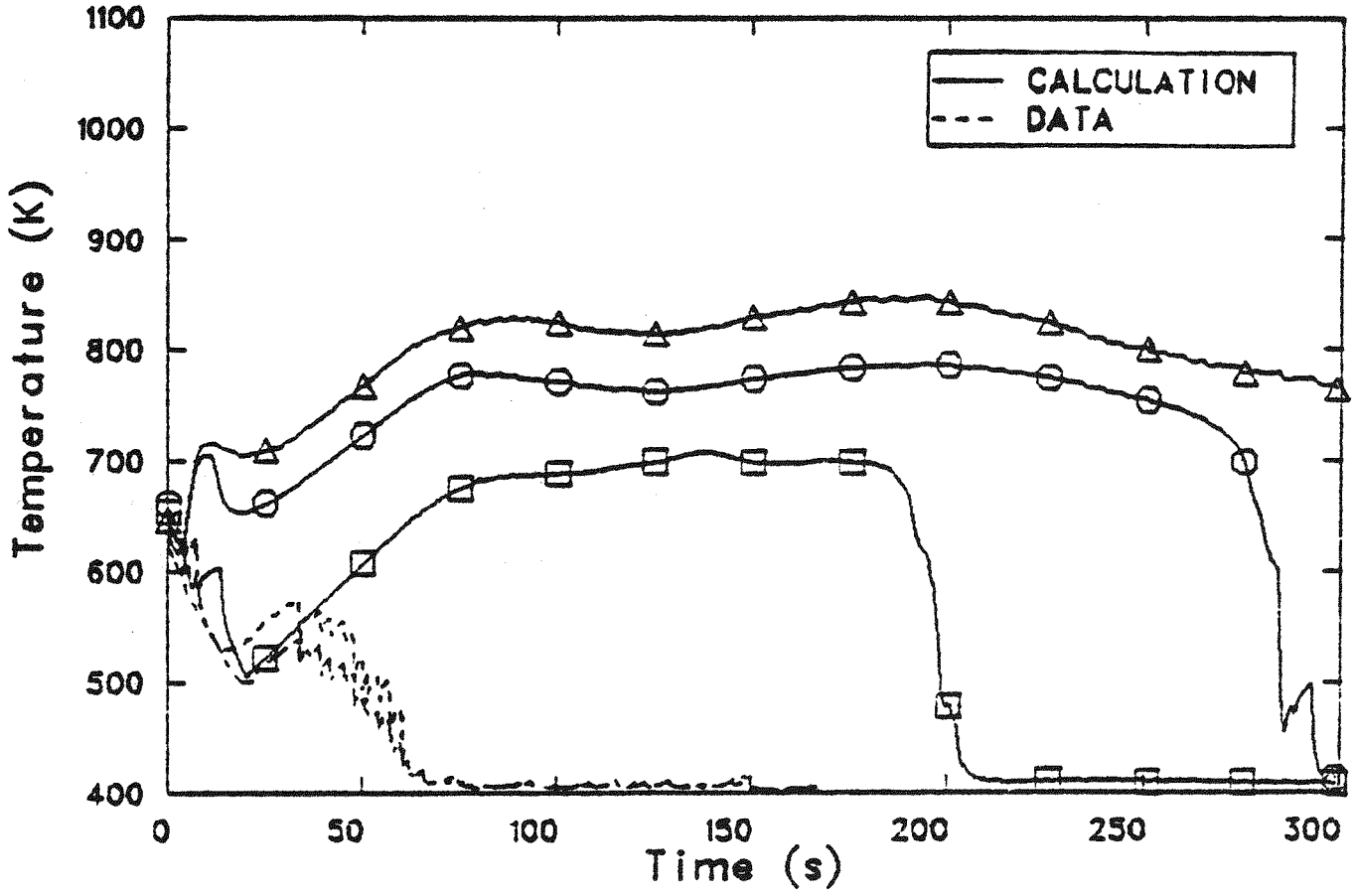

Figure 30. Calculated and measured cladding surface temperature response in the core upper region for Semiscale Mod-1 Test S-04-5.

Table 3. Times of critical heat flux, peak cladding temperatures, and quench for test S-04-5

Elevation[a] (m)	Power Step	Time of CHF		Time of PCT		Time of Quench	
		Measured (s)	Calculated (s)	Measured (s)	Calculated (s)	Measured (s)	Calculated (s)
0.0 - 0.152	1	0.0	1.0	48.0	7.0 - 8.0	100.0	60.0 - 61.0
0.152 - 0.280	2	0.5	0.5 - 1.0	48.0 - 61.0	7.0 - 8.0	105.0 - 115.0	79.0 - 80.0
0.280 - 0.407	3	0.5	0.5	60.0 - 70.0	7.0 - 8.0	160.0 - 200.0	98.0 - 100.0
0.407 - 0.534	4	0.5	0.5	8.50 - 61.0	7.0 - 8.0	230.0 - 235.0	118.0 - 120.0
0.534 - 0.788	5	0.5 - 2.5	0.5	8.00 - 92.0	7.0 - 8.0	245.0 - 300.0	135.0 - 155.0
0.788 - 0.915	6	0.5 - 3.5	0.5 - 2.5	80.0 - 192.0	8.0 - 56.8	No quench	113.0 - 128.0
0.915 - 1.042	7	3.0 - 4.0[b]	None - 3.0	70.0 - 193.0	0.0 - 7.5	210.0 - 275.0[c]	67.0
1.042 - 1.219	8	3.0 - 4.5[d]	None	135.0 - 195.0	0.0	210.0 - 295.0[e]	67.0
1.219 - 1.423	9	5.0[f]	None	0.0 - 11.0	0.0	75.0 - 120.0	79.0
1.423 - 1.676	10	None	None	0.0 - 72.0	0.0	95.0 - 110.0	77.0

a. Reference point is bottom of heated core.

b. One out of five thermocouples did not indicate CHF.

c. Three out of five thermocouples did not quench.

d. One out of four thermocouples did not indicate CHF.

e. One out of four thermocouples did not quench.

f. Three out of four thermocouples did not indicate CHF.

The calculated manometer-type oscillations were generally responsible for the quench time being too early at the higher elevations. Additionally, the initial calculated cladding temperature was above the minimum stable film boiling point (MFBP), which resulted in the time of quench being earlier than that measured.

The measured and calculated cladding temperature responses for Semiscale Mod-3 Test S-SB-2A are shown in Figures 40 and 41. The calculated maximum cladding temperature was 1230 K at 660 s, as compared to the measured peak cladding temperature of 800 K at 880 s. The reason for the difference between the two temperatures was attributed to an overestimate of the core power boundary condition in the calculation model. The core power was adjusted to account for system heat losses, which were overestimated in the initial conditions used in the calculation. The rate of cladding quench was correctly calculated, as was the location of CHF.

The measured and calculated cladding temperature responses for Semiscale Mod-3 Test S-SB-4 are shown in Figure 42. The calculated cladding surface temperature was in good agreement with the measured cladding surface temperature for the first 300 s. A 40-K heatup was calculated between 300 and 500 s, caused by a calculated vessel liquid level that decreased into the upper portion of the core (which was not observed in the test). A calculated accumulator injection at 480 s rapidly refilled the core, which resulted in the corresponding decrease in cladding surface temperatures. Subsequent calculations of additional accumulator injection resulted in further reductions in the cladding surface temperature after 500 s.

The mean difference and standard deviation between the calculated and measured peak cladding temperatures using the values from Tests K5A, S-04-5, S-28-1, S-28-10, and S-07-4 was -19.8 K $\pm$ 23.8 K. The calculated and measured data from Test S-SB-2A were not included, because the modeled core power

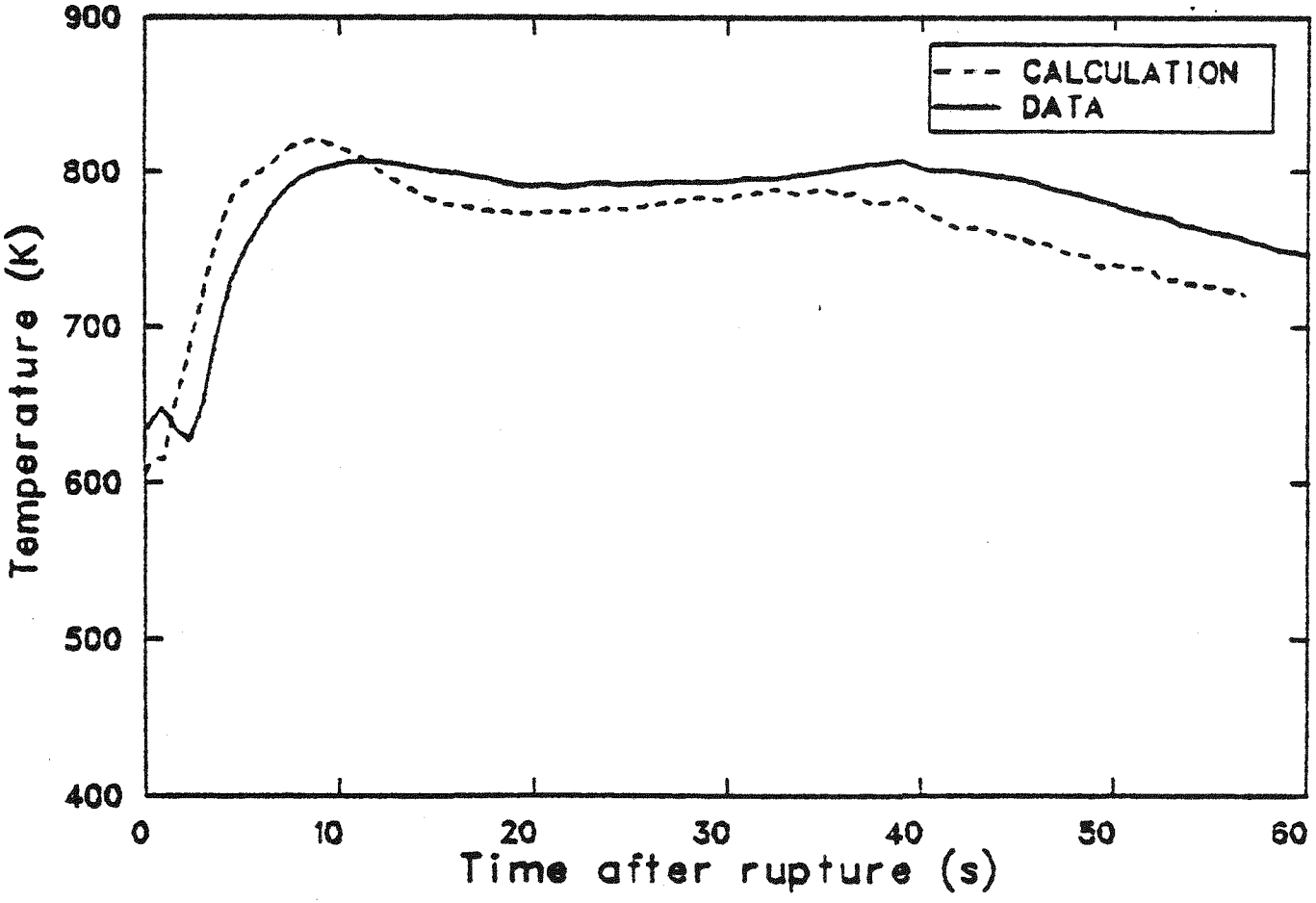

Figure 31. Calculated and measured cladding surface temperature response in the core lower region for Semiscale Mod-1 Test S-28-1.

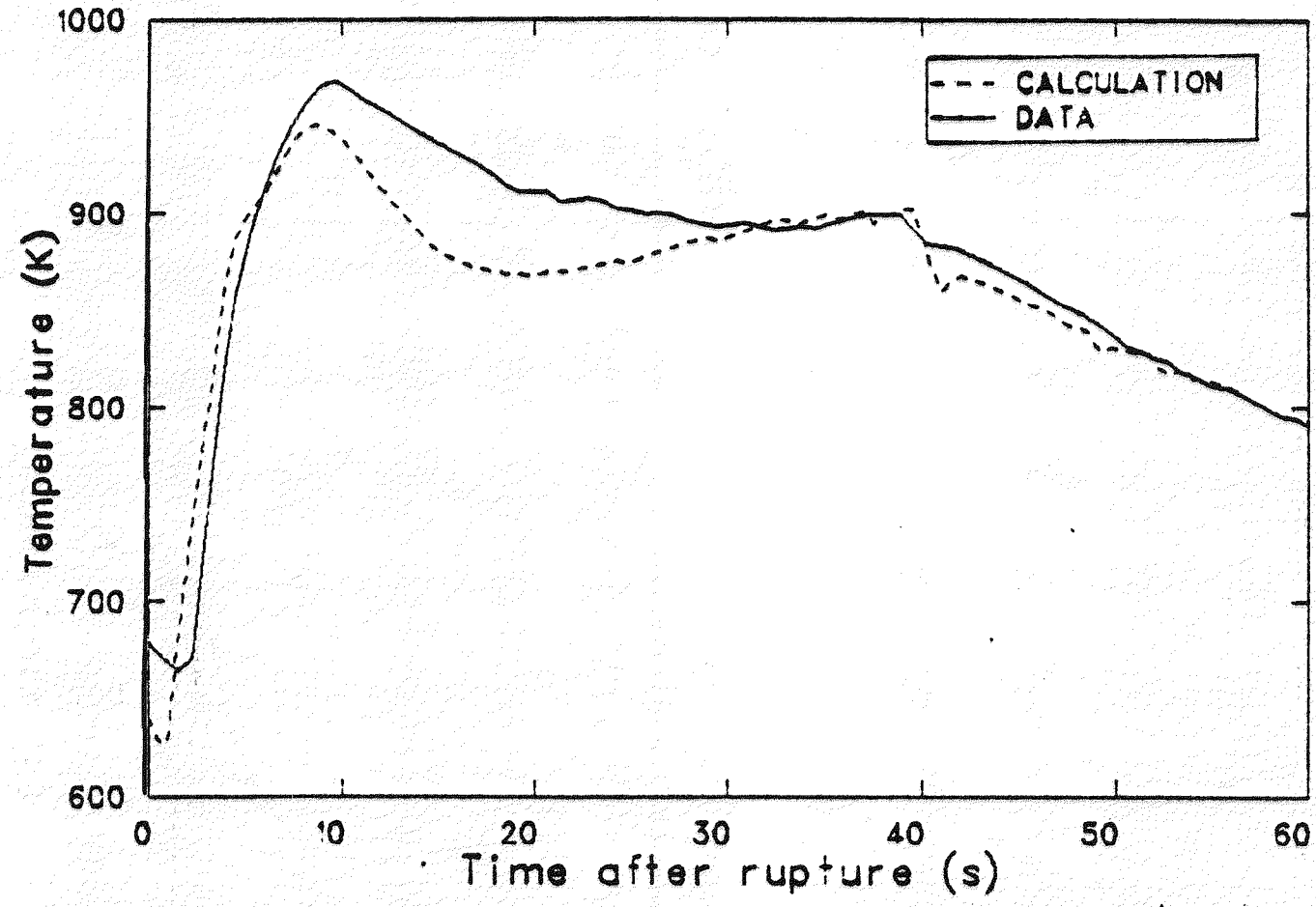

Figure 32. Calculated and measured cladding surface temperature response in the core middle region for Semiscale Mod-1 Test S-28-1.

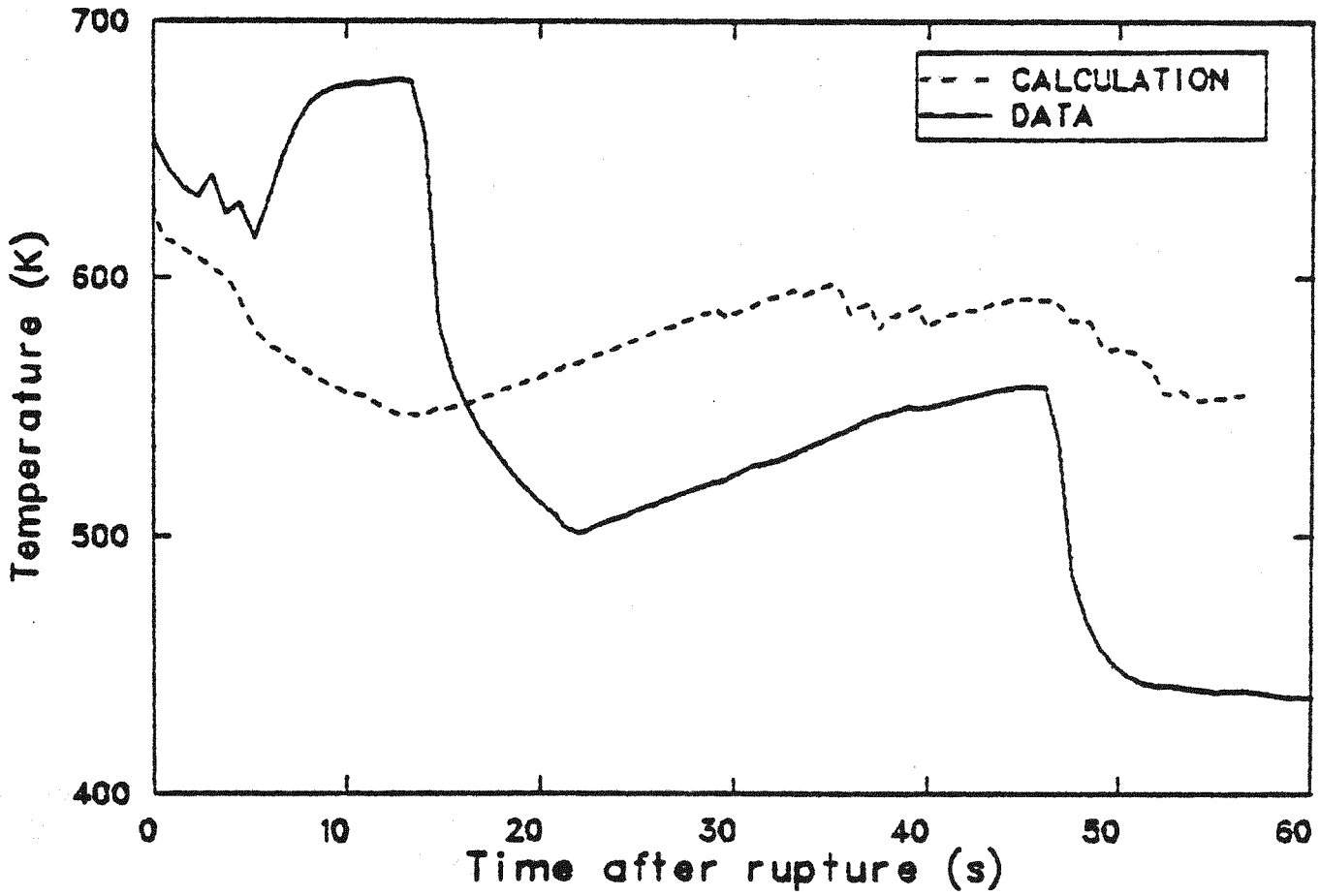

Figure 33. Calculated and measured cladding surface temperature response in the core upper region for Semiscale Mod-1 Test S-28-1.

Table 4. Maximum core temperature as a function of core level for Test S-28-1

Core/Level	Temperature (K)				
	Hot Rod	Rod 1	Rod 2	Rod 3	Rod 4
1 c[a]	725.8	728.6	714.0	715.5	712.4
m[b]	—	—	—	710.0	—
2 c	820.4	820.7	802.0	805.1	799.5
m	800.0	860.0	—	760.0	925.0
3 c	893.4	896.4	873.2	878.8	870.2
m	900.0	960.0	900.0	960.0	—
4 c	935.9	942.4	911.8	919.7	910.5
m	950.0	1010.0	900.0	1020.0	920.0
5 c	945.1	956.3	897.7	917.0	911.8
m	980.0	1000.0	970.0	1040.0	1020.0
6 c	831.3	888.9	818.0	803.3	845.6
m	—	—	910.0	920.0	875.0
7 c	641.5	711.3	639.5	639.5	658.3
m	—	780.0	750.0	790.0	760.0
8 c	637.8	668.9	635.8	635.8	635.8
m	—	630.0	680.0	—	670.0
9 c	630.3	628.5	628.5	628.5	628.5
m	620.0	—	600.0	—	600.0
10 c	616.0	614.8	614.8	614.8	614.8
m	—	—	—	600.0	—
11 c	599.9	599.6	599.6	599.6	599.6

a. Calculated.

b. Measured.

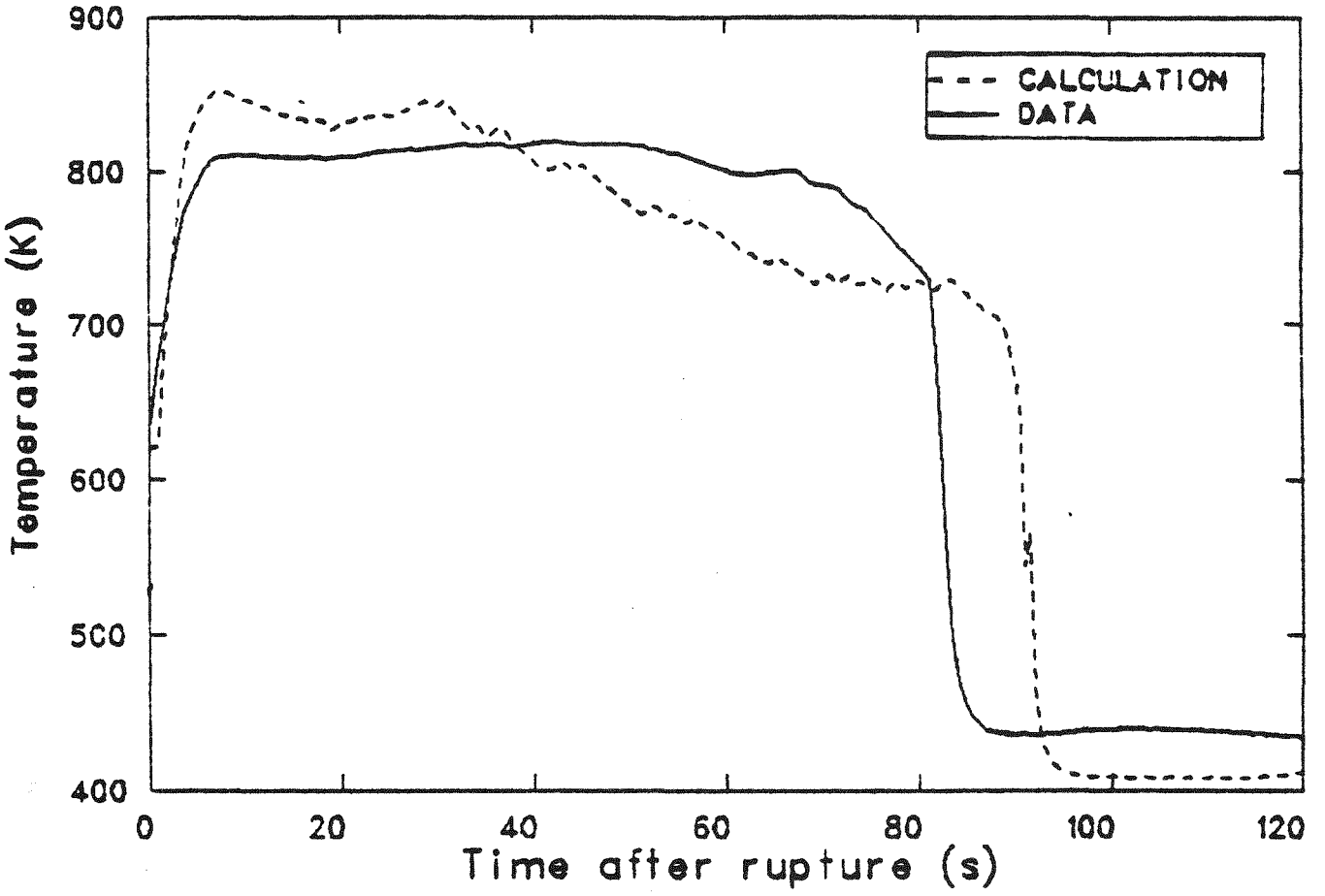

Figure 34. Calculated and measured cladding surface temperature response in the core lower region for Semiscale Mod-1 Test S-28-10.

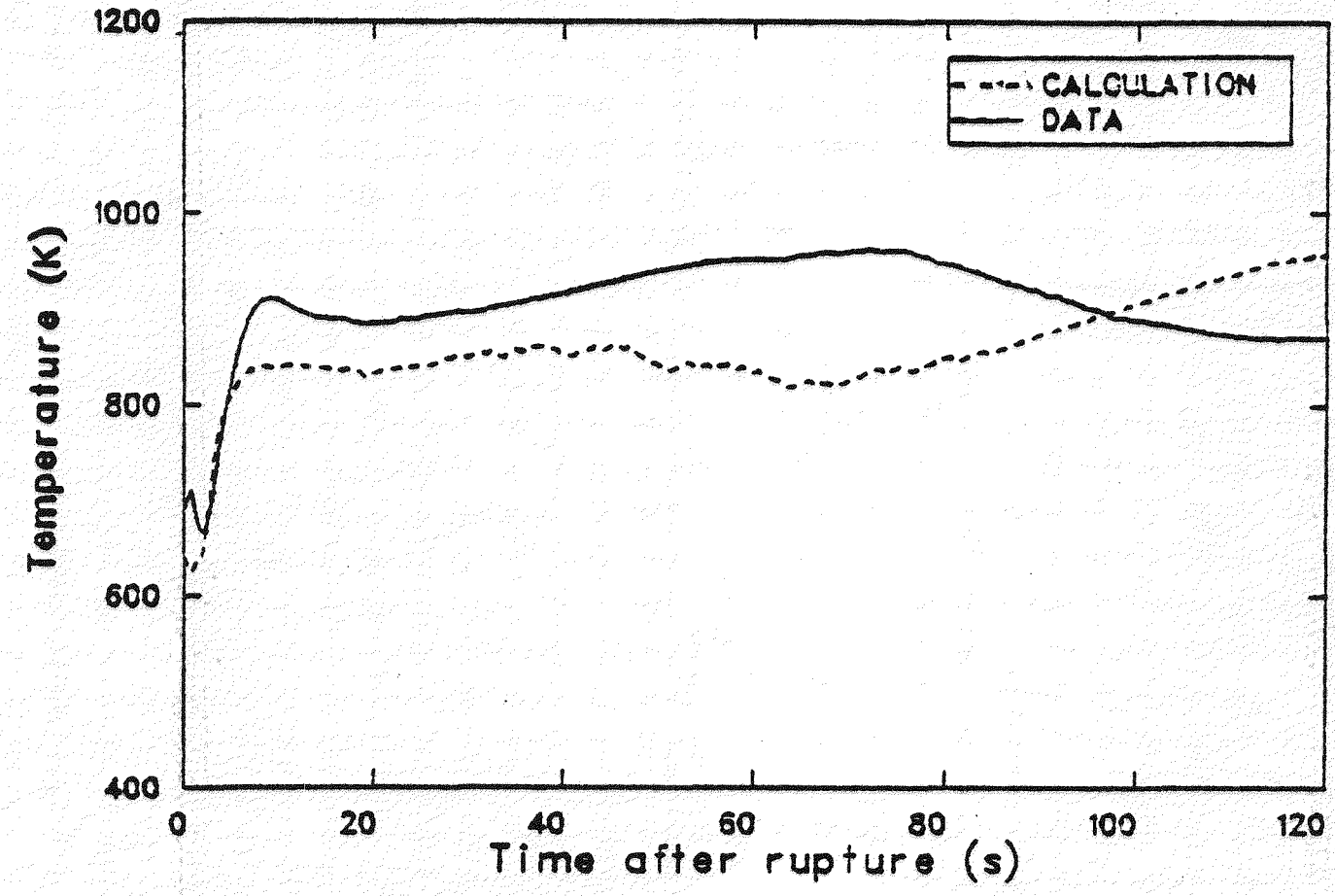

Figure 35. Calculated and measured cladding surface temperature response in the core middle region for Semiscale Mod-1 Test S-28-10.

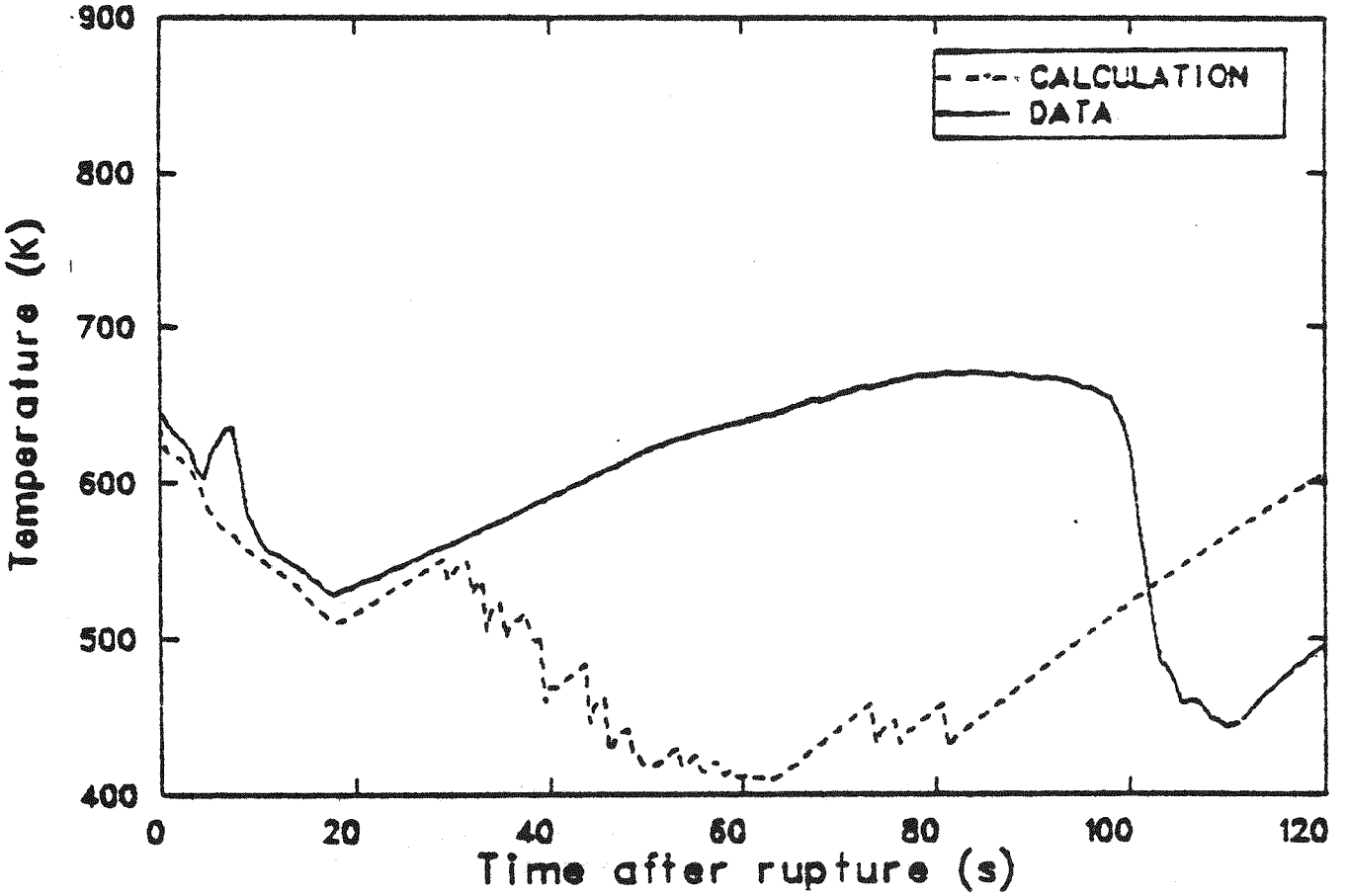

Figure 36. Calculated and measured cladding surface temperature response in the core upper region for Semiscale Mod-1 Test S-28-10.

Table 5. Quench time as a function of core elevation for Test S-28-10

	Time (s)				
Core/Level	Rod 1	Rod 2	Rod 3	Rod 4	Hot Rod
1 c[a]	37.5	35.0	35.0	35.0	35.0
m[b]	—[c]	—	70.0	—	—
2 c	60.0	54.0	50.0	50.0	50.0
m	80.0	—	80.0	90.0	80.0
3 c	90.0	80.0	67.0	80.0	78.0
m	100.0	100.0	100.0	—	100.0
4 c	115.0	107.0	98.0	107.0	105.0
m	110.0	110.0	110.0	100.0	110.0

a. Calculated.

b. Measured.

c. No data available.

was significantly overstated. By comparison of the two-sigma range of the temperature deviation (-43.6 K to 4.0 K) with the average peak temperature (~950 K) of the five tests, the largest temperature deviation was -4.5%. This deviation is greater than the measurement uncertainty of the cladding thermocouple, which is 2 to 5K up to 1800K. The consistently lower-than-measured peak cladding temperatures were apparently caused by consistent calculation of excessive liquid entrainment in the core prior to reflood. This resulted in delaying the time of CHF occurrence in the core, thereby allowing a longer period of cladding cooldown prior to post-CHF heatup. Overall, TRAC-PD2 appears to accurately calculate peak cladding temperatures given accurate modeling of break flow response.

Summaries of cladding temperature response are presented in Tables 6 through 9.

The conclusions regarding assessment of cladding temperature response are:

1. Cladding temperatures were generally well calculated when the occurrence of CHF was correctly predicted.
2. Condensation depressurization effects calculated by TRAC-PD2 tended to result in poor calculations of system mass distribution and cladding temperature response.
3. Calculations of system pressure response generally influenced the timing of accumulator injection, and consequently the timing of core reflood and quench was not well calculated.
4. The correlation for the MFBP was not generally applicable for the full range of conditions in the various calculations.
5. The occurrence of top-down and bottom-up quenches was adequately calculated, but the timing of the events and the cladding temperatures were inaccurate. The principal mechanism affecting the results of the calculation appeared to be excessive liquid entrainment in the core.
6. Cladding temperature response is dependent on correctly calculating the break mass flow rate and the amount of liquid entrainment in the core. The calculated cladding temperatures were generally lower than the corresponding measured temperatures.

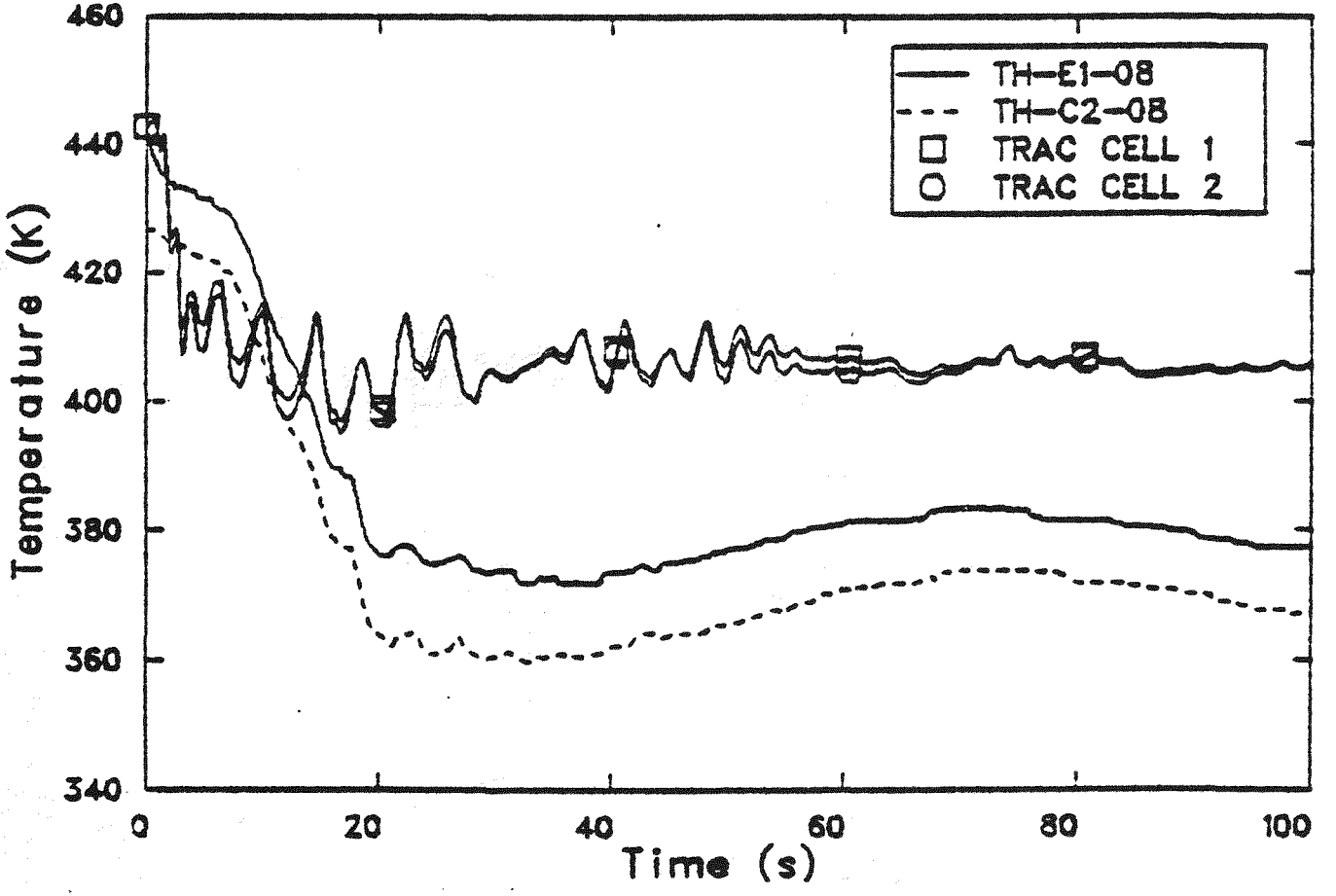

Figure 37. Calculated and measured cladding surface temperature response in the core lower region for Semiscale Mod-3 Test S-07-4.

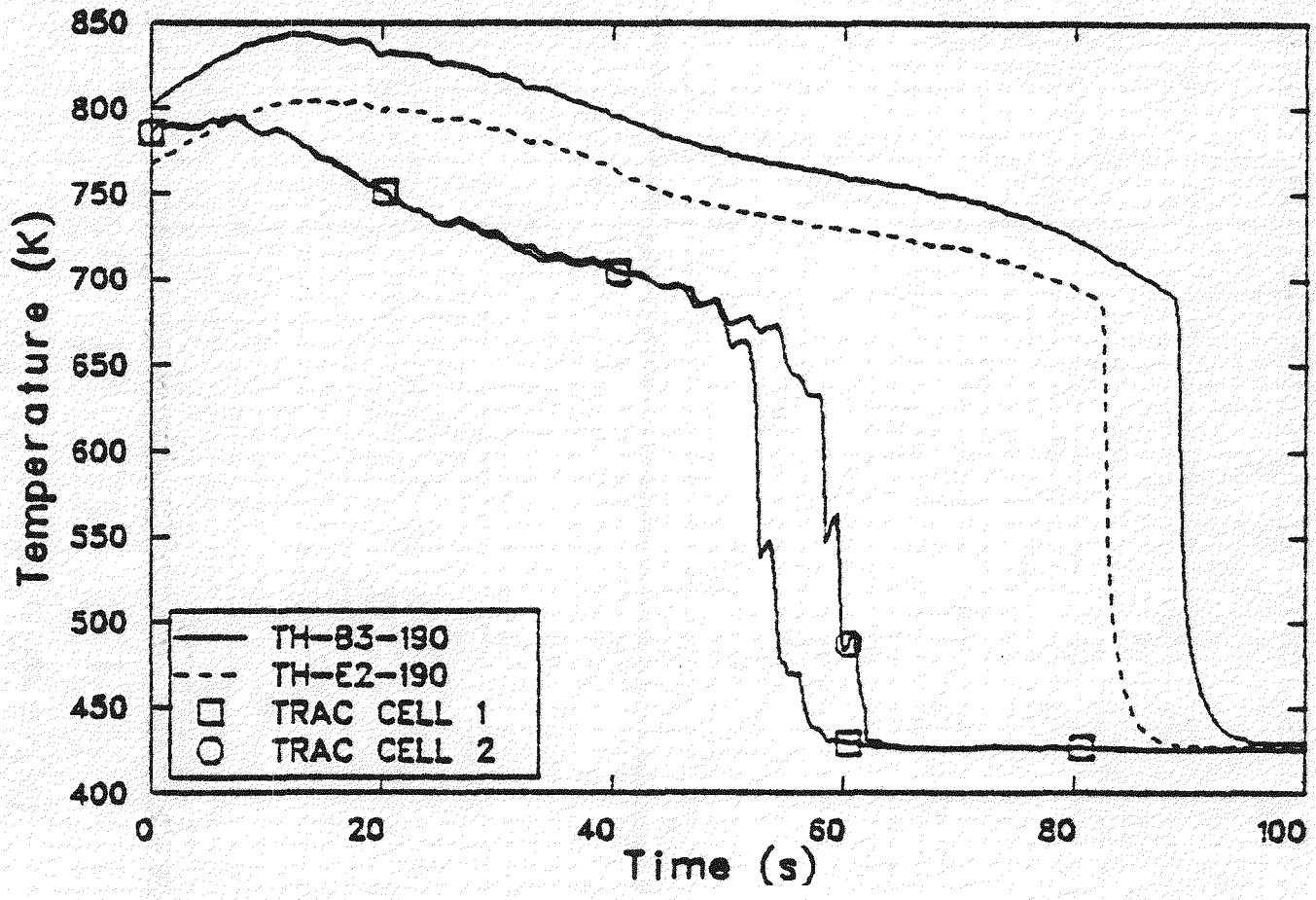

Figure 38. Calculated and measured cladding surface temperature response in the core middle region for Semiscale Mod-3 Test S-07-4.

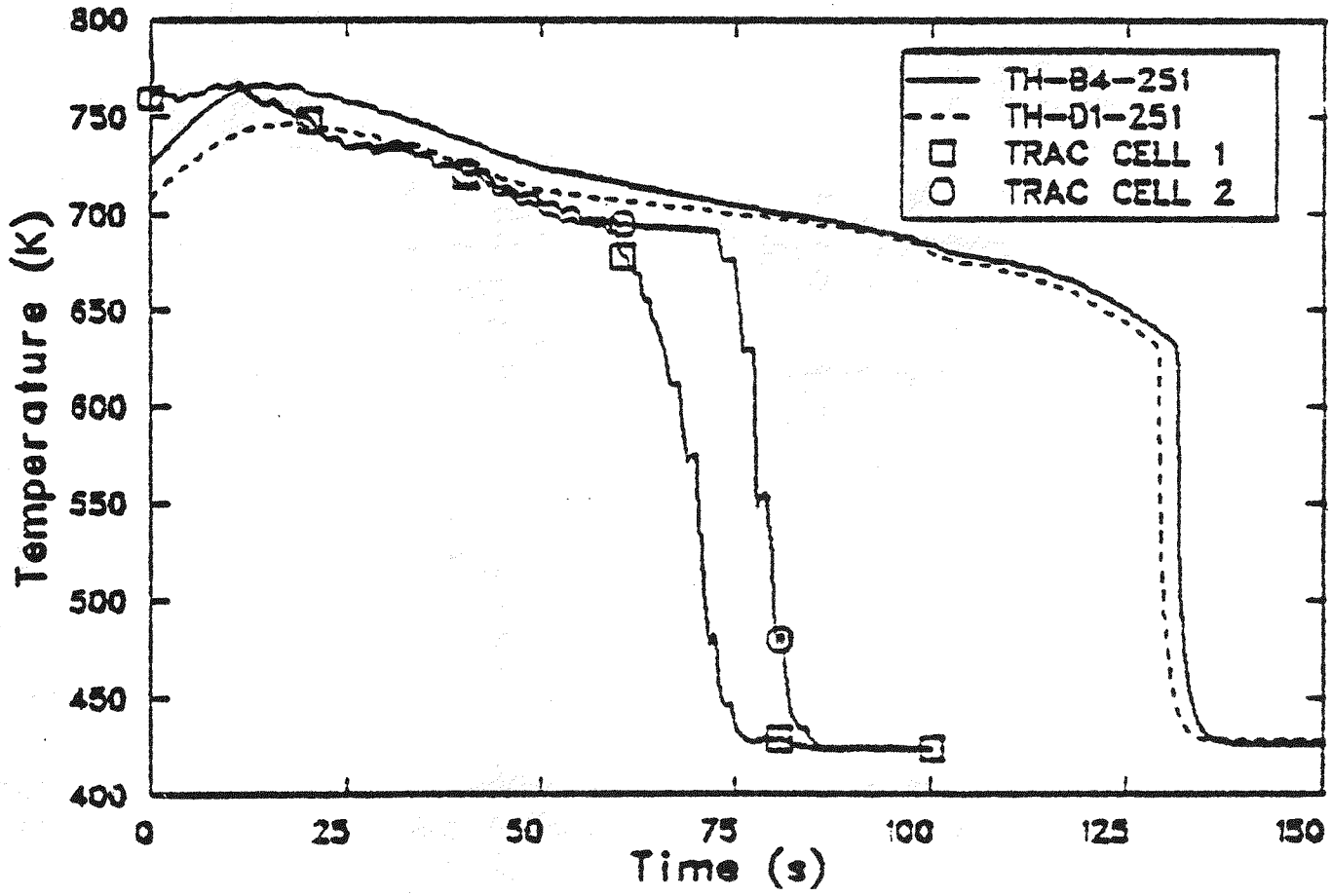

Figure 39. Calculated and measured cladding surface temperature response in the core upper region for Semiscale Mod-3 Test S-07-4.

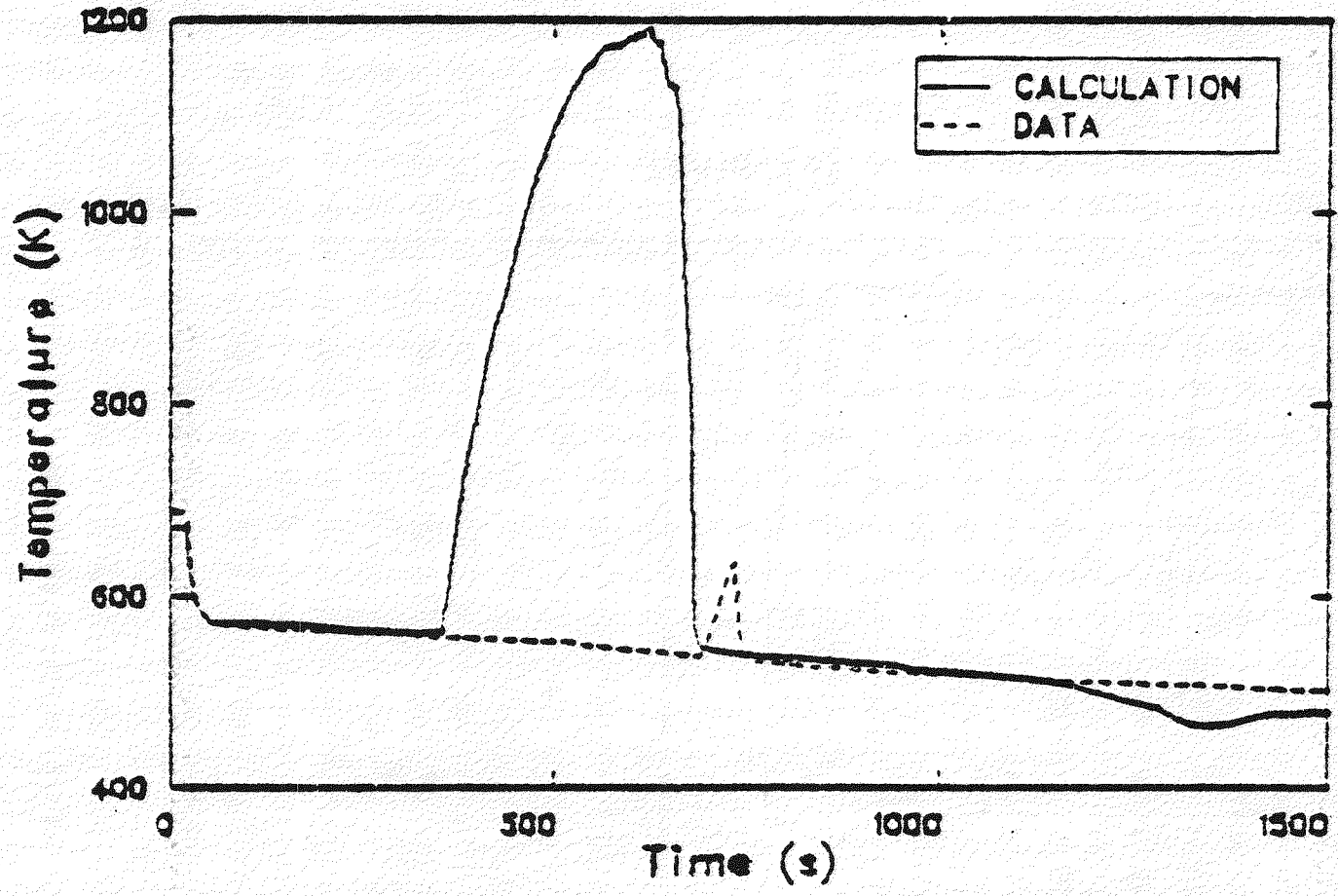

Figure 40. Calculated and measured cladding surface temperature response in the region where cladding heatup ended (1.52 to 2.13 m) for Semiscale Mod-3 Test S-SB-2A.

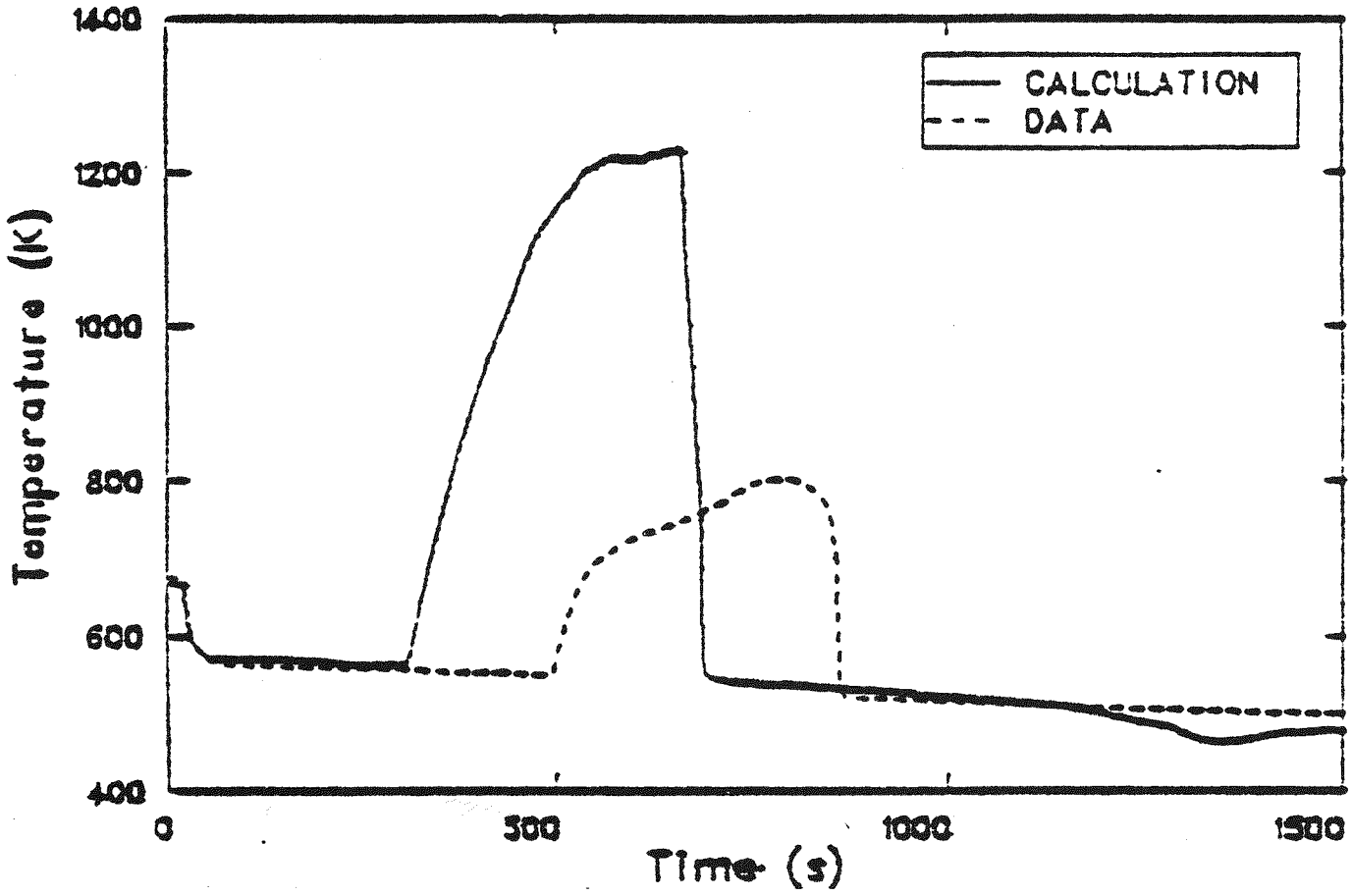

Figure 41. Calculated and measured cladding surface temperature response in the region of maximum cladding temperature (2.43 to 2.74 m) for Semiscale Mod-3 Test S-SB-2A.

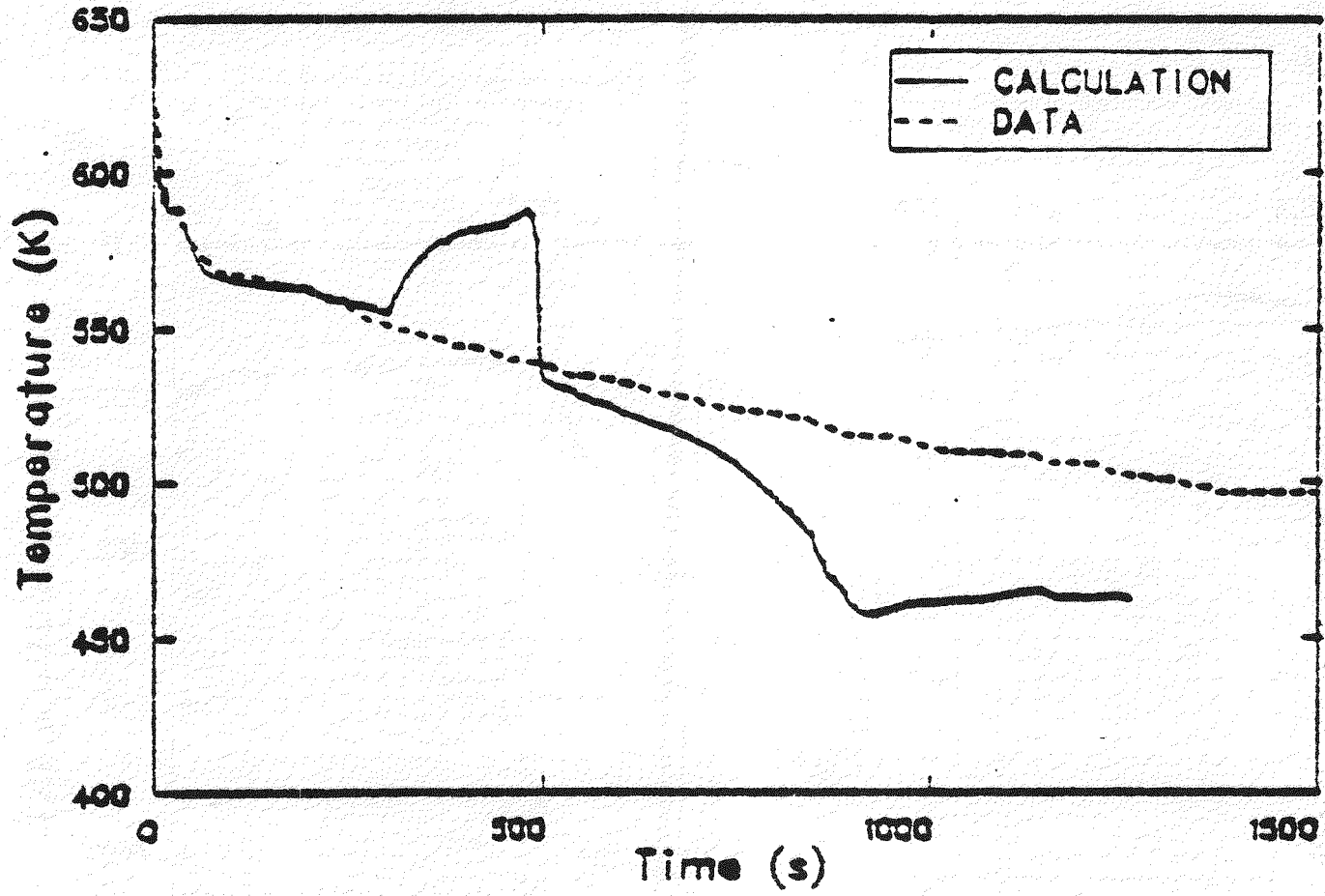

Figure 42. Calculated and measured cladding surface temperature response in the core upper region for Semiscale Mod-3 Test S-SB-4.

Table 6. Calculated and measured times of critical heat flux at the hot spot

Test	Calculated (s)	Measured (s)	Difference (s)
S-04-5	1	3	-2
S-28-1	1	2.5	-1.5
S-28-10	2	2.5	-1.5
S-SB-2A	302	492	-190

Table 7. Calculated and measured peak cladding temperatures

Test	Calculated (K)	Measured (K)	Difference (K)
K5A	982	975	7
S-04-5	950	980	-30
S-28-1	945	980	-35
S-28-10	977	983	-6
S-07-4	785	820	-35
S-SB-2A	1230	800	430

Table 8. Calculated and measured times of peak cladding temperatures

Test	Calculated (s)	Measured (s)	Difference (s)
K5A	100	100	0
S-04-5	8	10	-2
S-28-1	8.5	10	-1.5
S-28-10	120	75	45
S-07-4	7	11	-4
S-SB-2A	660	880	-220

Table 9. Calculated and measured times of hot spot quench

Test	Calculated (s)	Measured (s)	Difference (s)
K5A	250	250	0
S-04-5	155	290	-135
S-28-1	50	43	7
S-28-10	105	110	-5
S-07-4	60	92	-32
S-SB-2A	659	834	-175

4. RUN TIME STATISTICS

Statistics regarding the CPU time, transient time, and the ratio of CPU time to transient time (CPU/real) are summarized in Table 10. The data were obtained from four of the Semiscale assessment calculations, Test S-04-5 (Appendix B), Test S-07-4 (Appendix D), and Tests S-SB-2A and S-SB-4 (Appendix E). Tests S-28-1 and S-28-10 were terminated early because of very slow run times, but no data were available. Data were also not available in the PKL K5A test (Appendix A). The highest ratios of CPU time to transient time occurred during the reflood phase of the calculations. The combination of rapid phase changes coupled with changes of the velocity vectors was apparently the dominant mechanism responsible for the high CPU ratios.

Table 10. Run time statistics

Test ID	CPU Time (s)	Transient Time (s)	CPU/Real
S-04-5	49166	166.64	295.0
S-07-4	7939	100.00	79.4
S-SB-2A	43080	1500.00	28.7
S-SB-4	16270	1260.00	12.9

5. USER EXPERIENCES

User experiences gained from the various calculations described in this report are summarized in this section. These experiences may be subdivided into three separate categories; development of TRAC-PD2 test facility models, steady-state initialization, and transient calculation.

5.1 Development of TRAC-PD2 Test Facility Models For LBLOCA Calculations

The ECC water temperature should be linearly ramped from saturation to the desired subcooled temperature over 5-10 s to avoid condensation problems at the onset of ECC injection.

The intact loop accumulator trip number and the intact loop low pressure injection (LPIS) trip number should be greater than 1000. Trips that are greater than 1000 cause the code to reduce its time-step size to the minimum value by the trip rather than having TRAC-PD2 internally reduce the time-step size. This results in a smoother running calculation with less frequent termination caused by time-step reduction problems or outer iteration problems.

The user should perform sensitivity calculations to determine the break nozzle nodalization. A 17-cell nodalization is recommended in the TRAC-PD2 newsletters. Use single-phase data when performing sensitivity calculations, because the two-phase data is generally inadequate for comparison purposes.

The material properties used by TRAC-PD2 for thermal conductivity and volumetric heat capacity are internally generated. The values used for boron nitride, which is a typical material used in electrical heater rods, are based on data reported in 1976. Newer information has since been developed by the Semiscale program which updates the original data (Reference 11 of Appendix E). Specifically, the new information yields lower values for conductivity and heat capacity than TRAC-PD2 calculates. No significant difference in cladding temperatures or stored energy should occur at boron nitride temperatures below 925 K. However, for calculations where significant heatup is expected or for calculations using as a data base facilities where insulators other than boron nitride are used, the option for user input material properties is necessary to adequately predict heater rod thermal response.

The check valve on the accumulator is tripped open when the system pressure decreases below the accumulator pressure. If there is a primary system pressure increase after the check valve opens, there could be a period when the check valve could rapidly open and close. During this period, the code might be required to use very small time steps and still have a failure caused by convergence problems. To bypass this problem, the valve should be modeled to stay open until tripped to close.

5.2 Steady-State Initialization

The same temperature and pressure can be specified in all the primary system components, and TRAC-PD2 can be used to calculate the steady-state pressure and temperature distribution. This distribution will likely not be exactly the desired condition; however, the steam generator secondary system pressure and feedwater flow rate can then be adjusted to bring the primary conditions into the desired range. A word of caution: this technique of arriving at the desired steady state can result in steam generator secondary conditions that may be outside the desired limits. If secondary-system conditions are important, some compromise between secondary and primary conditions may be required.

5.3 Transient Calculations

In the event of severe convergence problems which can occur during reflood, the convergence criteria should be restricted to the smaller of the recommended values and the maximum allowable time-step size reduced. These criteria can be lifted after the calculation gets through the problem area.

The vessel conditions can be more accurately calculated using a direct matrix inversion (explicit). However, the vessel conditions can be calculated with nearly the same accuracy using a semi-implicit scheme. The semi-implicit method is recommended, because it is faster for a large vessel model.

All trip signals are set by the code during the initial transient calculation. In subsequent restart calculations, these trips are no longer required as input. In fact, the presence of trip data in the transient restart calculation will reset the trip initiation time back to zero, which causes errors in those trip signals using time as a reference parameter.

When the core is completely voided, use the Iloeje correlation for the DNB temperature. The difference in the Iloeje temperature and the homogeneous minimum nucleation temperature is slight and will not affect the cladding temperature response prior to the reflood portion of the calculation. Using the Iloeje correlation can reduce the cost of the calculation up to 50% prior to this phase of the calculation. Use the homogeneous minimum nucleation temperature during the reflood portion of the calculation.

6. CONCLUSIONS

Conclusions regarding the calculation of break flow rate response, primary system pressure response, core flow rate response, and cladding temperature response are presented in this section. In general, TRAC-PD2 calculated the LBLOCA primary system responses reasonably well based upon the criteria used in this report to judge the code. It is therefore considered adequate for LBLOCA calculations. However, primary system mass distribution was not adequately calculated in the small-break calculations, which had an adverse effect on other important parameters. Consequently, use of TRAC-PD2 for SBLOCA calculations is not recommended.

6.1 Conclusions Regarding Break Flow Rate Response

1. TRAC-PD2 break flow calculations were sensitive to model nodalization.

2. Break flow calculations were very sensitive to initial conditions in the blowdown piping.

3. Consistent inaccuracies in break flow rate response were not found to occur in all the calculations. Break flow was too high in the small-break calculation (by inference from the calculated primary system mass inventory) and was too low in the PKL K5A, S-28-1, and S-28-10 calculations.

4. Modeling of the break downstream conditions and nodalization of the break upstream volume geometry appear to be the most significant factors in accurately calculating the break flow response.

6.2 Conclusions Regarding Primary System Pressure Response

1. Inaccurate modeling of the break geometry (incorrect friction factors, inadequate nodalization, and failure to specify a reasonable set of discharge coefficients) caused inaccuracies in the calculation of break flow rate and, consequently, in the rate of primary system depressurization.

2. Mass distribution in the primary coolant loops influenced the time of accumulator injection initiation and, consequently, the primary system pressure response.

3. The subcooled depressurization phase is adequately represented by TRAC-PD2.

4. The *general* trends in the calculated pressure response data are reasonably specified by TRAC-PD2 during the saturated blowdown phase, although large deviations in the pressures (up to 100%) were calculated. The mean maximum deviation was +55% during saturated depressurization in the LBLOCA calculations.

5. Primary system pressure response was most significantly affected by the break flow rate response, and calculations of condensation depressurization events generally overstated the pressure response.

6.3 Conclusions Regarding Core Flow Rate Response

1. Excessive condensation depressurization in the top of the downcomer resulted in periods of poor agreement with core flow data in several of the calculations, which indicates some problems may arise in the calculation of core reflooding using modeled ECC systems.

2. Downcomer hot wall delay effects are sensitive to heat structure modeling of the effective thickness. Hot wall delay effects can be increased if the effective thickness is greater than the actual effective thickness.

3. Calculation of coolant mass distribution during S-SB-2A significantly affected the results. The calculated mass in the broken loop pump seal was not retained in the system as it should have been, which affected the core flow response. The problem of calculating the correct mass distribution indicates that TRAC-PD2 should not be used for SBLOCA calculations, because incorrectly calculated system mass distribution affects core temperature response.

4. Core flow response was generally accurate; however, some inadequacies regarding liquid entrainment were calculated. The significant differences in break flow response caused some problems regarding ECC injection timing.

6.4 Conclusions Regarding Cladding Temperature Response

1. Cladding temperatures prior to cladding quench were adequately calculated when the time of CHF was correctly calculated. Excessive liquid entrainment resulted in some of the peak cladding temperatures being lower than the corresponding measured values.

2. Condensation depressurization effects tended to be overstated by TRAC-PD2, resulting in inaccurate calculations of primary system mass distribution and cladding temperature response.

3. Calculations of system pressure response generally influenced the timing of accumulator injection, and consequently the timing of core reflood and quench was not adequately calculated.

4. The cladding temperatures prior to the top-down and bottom-up quenches were adequately calculated, but the times of quench were generally inaccurate.

5. Cladding temperature response is dependent on correctly calculating the break flow rate, mass distribution, and liquid entrainment in the core. Condensation in the top of the downcomer can reduce the primary system pressure. This in turn can lead to early initiation of ECC injection, thereby causing early quench of the fuel rods.